

Landforms and landscape evolution in the Skardu, Shigar and Braldu Valleys, Central Karakoram

Yeong Bae Seong^{a,*}, Michael P. Bishop^b, Andrew Bush^c, Penny Clendon^d, Luke Copland^e, Robert C. Finkel^f, Ulrich Kamp^g, Lewis A. Owen^a, John F. Shroder^b

^a Department of Geology, University of Cincinnati, P.O. Box 0013, Cincinnati, OH 45221-0013, U.S.A.

^b Department of Geography and Geology, University of Nebraska – Omaha, 6001 Dodge Street, Omaha, NE 68182-0199, U.S.A.

^c Department of Earth and Atmospheric Sciences, University of Alberta, 1-26 Earth Sciences Building, Edmonton, Alberta, Canada T6G 2E3

^d Department of Geography, University of Canterbury, Private Bag 4800 Christchurch, New Zealand

^e Department of Geography, University of Ottawa, Ottawa, Ontario, Canada K1N 6N5

^f Center for Accelerator Mass Spectrometry, Lawrence Livermore National Laboratory, Livermore, CA 94550, USA

^g Department of Geography, The University of Montana, SS 204, Missoula, MT 59812-5040, U.S.A.

ARTICLE INFO

Article history:

Accepted 15 November 2007

Available online 10 May 2008

Keywords:

Central Karakoram

Glacier erosion

Landscape evolution

Terrestrial cosmogenic nuclide (TCN)

exposure dating

Glaciation

Paraglaciatio

Outburst flood deposits

Late Quaternary

ABSTRACT

The Central Karakoram, which includes K2 in Pakistan, is one of the most rapidly rising areas on Earth and exhibits complex topography and extreme relief. Impressive valley fills and glacial landforms are present throughout the valleys. The dynamics of landscape evolution of the region are currently not well understood. Consequently, the landforms were mapped and assessed in the Skardu, Shigar, and Braldu valleys, to elucidate the spatio-temporal scale dependencies of surface processes active in the region. These valleys were examined using geomorphic field methods, remote sensing, geomorphometry, and terrestrial cosmogenic nuclides (TCNs) surface exposure dating. The glaciers in this region have oscillated considerably throughout the Late Quaternary, and four glacial stages have been recognized including at least six glacial advances. Surface processes readjusted after glacier retreat, and ubiquitous mass movements and catastrophic landsliding transported material from steep slopes to valley bottoms, while glaciofluvial meltwater and glacier outburst floods redistributed sediment down valley. Glacier geochronology and late Holocene ages of the outburst flood deposits indicate that landscape evolution has been dominated by glaciation and paraglaciation during the late Quaternary.

© 2008 Elsevier B.V. All rights reserved.

1. Introduction

The Central Karakoram is an area of significant anomalous topography, home to more than sixty peaks that rise above 7000 m above sea level (asl) with four of these peaks exceeding 8000 m asl. The mountain range is one of the most rapidly rising, with rates of uplift estimated to be between 2 and 6 mm a⁻¹ (Rex et al., 1988; Searle et al., 1990; Foster et al., 1994; Leland et al., 1998). The origin of the topography of the Central Karakoram, however, is currently not well understood, although the erosion/uplift feedback mechanism is now recognized as a likely primary controlling factor (Searle, 1991; Pinter and Brandon, 2005). Globally-significant interactions between climate, surface processes, and tectonics have recently been proposed to explain climate change and mountain building (Raymo et al., 1988; Molnar and England, 1990; Koons 1995; Avouac and Burov, 1996). Much research has focused on climate versus tectonic forcing

(Raymo et al., 1988; Molnar and England, 1990) and the dominant surface processes responsible for relief production and topographic evolution (Montgomery, 1994; Burbank et al., 1996; Brozovic et al., 1997; Whipple and Tucker, 1999). Furthermore, Brozovic et al. (1997) suggested that where mountain belts intersect the snowline, glacial and periglacial processes place an upper limit on altitude, relief, and the development of topography irrespective of the rate at which tectonic processes operate.

The influence of glaciation, mass movement, and fluvial erosion on the relief structure of the western Himalaya has not been thoroughly evaluated (Bishop et al., 2002, 2003). Understanding the differential influence of surface processes on production of relief will require research to address the issues of polygenetic topographic evolution, operational scale of individual surface processes, operational scale at which landscape denudation affects the macroscale tectonic influx of mass (Bishop and Shroder, 2000; Bishop et al., 2002), as well as evaluation and coupling new erosion models that account for internal and external forcing. Furthermore, it is essential that field-based studies and landform mapping be used to elucidate the complex interplay of surface processes that are responsible for the sediment evacuation and govern the magnitude of denudation.

* Corresponding author.

E-mail address: ybseong@hotmail.com (Y.B. Seong).

¹ Present address: Department of Earth and Environmental Sciences, Korea University, Anam-Dong, Seongbuk-Gu, Seoul, 136-704, Korea.

Denudation by mass movement in the Himalaya is also known to be pervasive (Burbank et al., 1996; Shroder, 1998; Shroder and Bishop, 1998) and during interglacial times may be the dominant process on the mountain landscape. Primary shear surfaces of bedrock are at high angles on mountain-tops and generally decrease with altitude unless they pass downward in scale-dependently controlled sacking, listric faults, or ductility at depth (Shroder and Bishop, 1998). Secondary shear surfaces are ubiquitous from post-failure weathering, creep and minor slope processes. Primary and secondary shear surfaces can be overlooked in broad-brush approaches using DEM slope analysis that may not differentiate depositional slopes at the angle of repose. During glacial times, mass movement from high-altitude undercut slopes may be most important, whereas during deglaciation, failure of unsupported rock slopes may be more important.

Identifying and mapping the landforms along with geochronological data can provide an assessment of the role of climate forcing and glaciation in the landscape evolution. Significant changes in climate and glaciation, for example, can occur over a relatively short time period, and glaciers are likely to be primarily responsible for significant denudation of the landscape. Furthermore, upon deglaciation, surface processes readjust to new environmental conditions that result, for example, by landsliding, erosion and glacier lake outburst floods. Defining the magnitude, frequency and roles of these processes is a first step in quantifying and understanding the dynamics of glaciation and landscape evolution in high mountains.

The Central Karakoram, near K2 in Pakistan, exhibits complex topography and an intricate interplay of surface processes that provides one of the best natural laboratories to begin to examine the relationships between climate, glaciation and landscape evolution. Surprisingly, the impressive landforms, such as moraines, alluvial fans, flood deposits, are present within the valleys and intermontane basins have received little study and published studies, present conflicting interpretations of landform features (e.g., moraines versus rock avalanche; Owen, 1988; Hewitt, 1998, 1999; Seong et al., 2007). In addition, the timing of geomorphic events that significantly govern landscape evolution in selected portions of the western Himalaya was not clearly understood. Consequently a need exists for geomorphological mapping and geochronological assessment of the dynamics of landscape evolution near K2. Our research, therefore, focused on describing the morphology of the major valleys between Skardu and K2 in the Central Karakoram to assess a multitude of processes that are responsible for erosion, transportation and sedimentation by way of glacier, hillslope and river. Terrestrial cosmogenic nuclide (TCN) surface exposure dating is applied to define the age of landforms produced by glacial and associated processes. Collectively the results are synthesized to develop a conceptual model of landscape evolution for this region.

2. Study area

The Skardu, Shigar, and Braldu valleys are located in the Central Karakoram, which is situated at the western end of the Transhimalaya

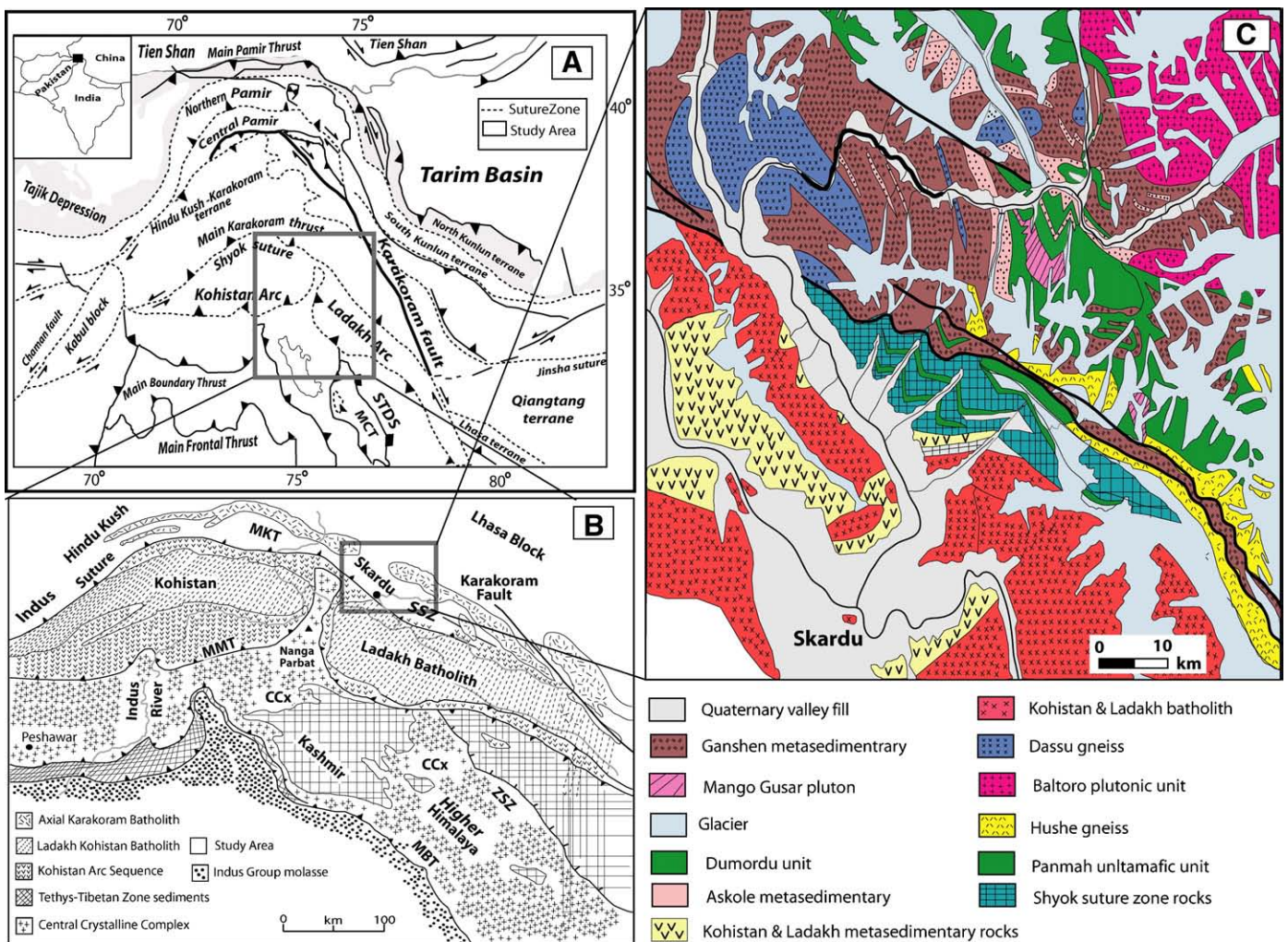


Fig. 1. Geologic context of the study region. (A) Tectonic map of the western end of the Tibetan-Himalayan orogen, modified from Robinson et al. (2004). STDS-South Tibetan Detachment, MCT-Main Central Thrust (B) Geologic map of the Central Karakoram (after Parrish and Tirrul, 1989). MBT-Main Boundary Thrust, CCx-Central Crystalline Complex of Higher Himalaya, ZSZ, Zaskar Shear Zone, MMT-Main Mantle Thrust, MKT-Main Karakoram Thrust, SSZ-Shyok Suture Zone, AKB-Axial Karakoram Batholith, and BG-Baltoro Granite. (C) Geological map of study area (adapted from Searle, 1991).

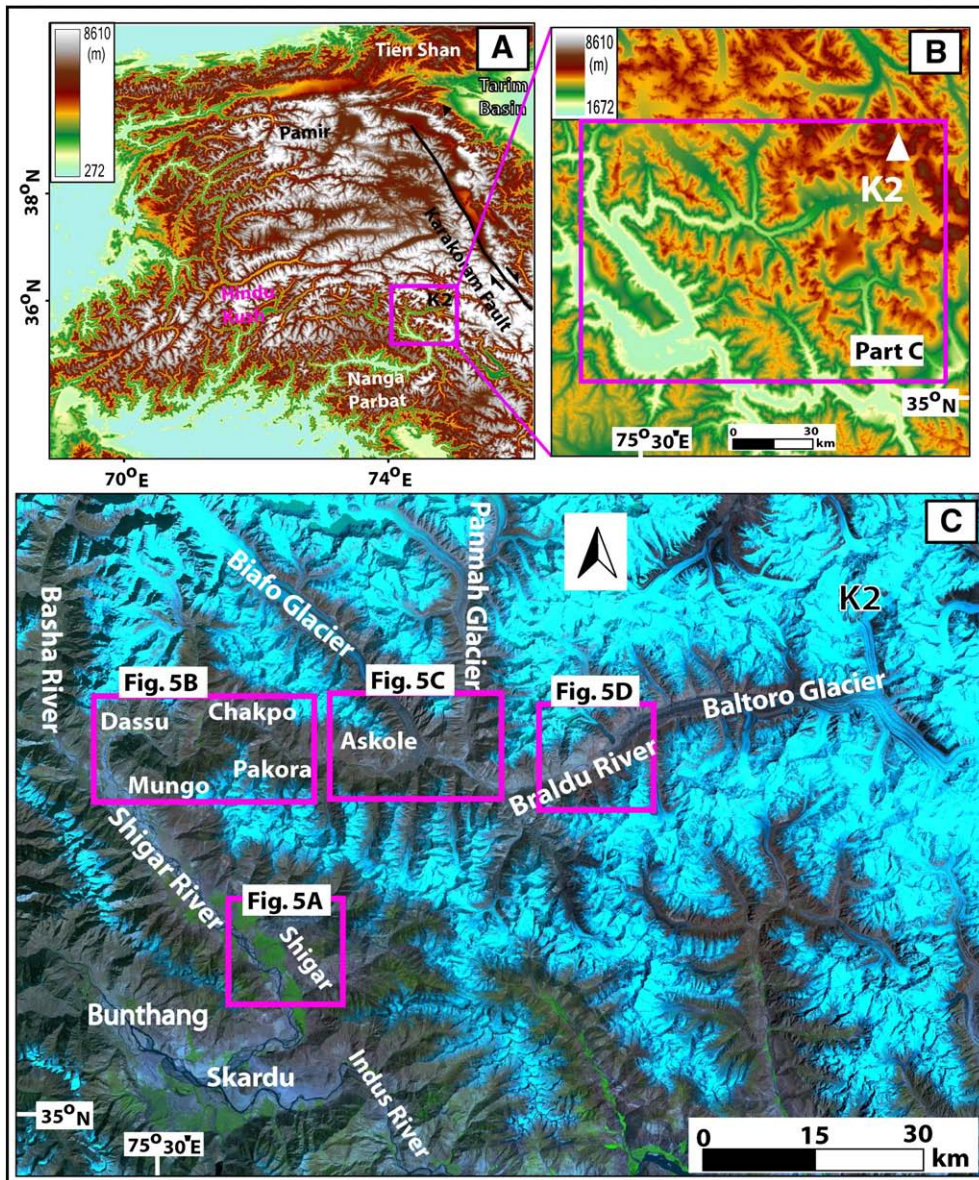


Fig. 2. Topography of western Tibet (A), the Central Karakoram (B) (Altitudes ranges from 1652 m asl in valley floor to 8611 m asl in K2 peak) and Satellite (ETM+) image showing the topography and the glaciers in the study area (C).

(Fig. 1). This region exhibits extreme relief, extensive glaciation, and ubiquitous mass movements. Rates of denudation are thought to be high in this region given the extensive relief, with valley floors averaging 2000 m asl and peaks rising to >7 km from low lying valleys (Fig. 2).

The hypsometry of the region is such that ~80% of the land area lies between 3000–6000 m asl, although this relief represents ~50% of the total relief from 2000 to >8000 m asl (Fig. 3). Altitude below 3000 m asl are coincident with the submontane zone by Hewitt (1989), where fluvial and eolian processes dominate and valley bottoms are covered by glacial and glaciofluvial sediments and slope deposits, with thin veneers of eolian sediment including loess and dune deposits. Intermediate altitudes have been characterized by Hewitt (1989) as subalpine and high alpine zones. Active paraglacial processes and postglacial rock debuttracing-induced landslides, and outburst floods occur in the lower altitudes of this zone. Glaciers and snow fields become more dominant with increased altitude. The perennial ice and climate zone at high altitude comprises the very highest ridges and peaks including K2 (8611 m asl), Gasherbrum 1 (8068 m asl), Broad Peak (8047 m asl), and Gasherbrum II (8035 m asl). Glacio-nivation and snow avalanching are dominant surface processes.

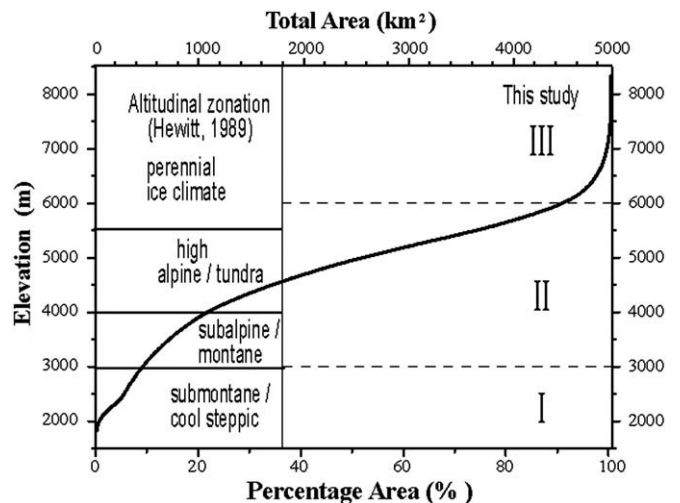


Fig. 3. The distribution of altitudes for the Central Karakoram plotted on a hypsometric curve.

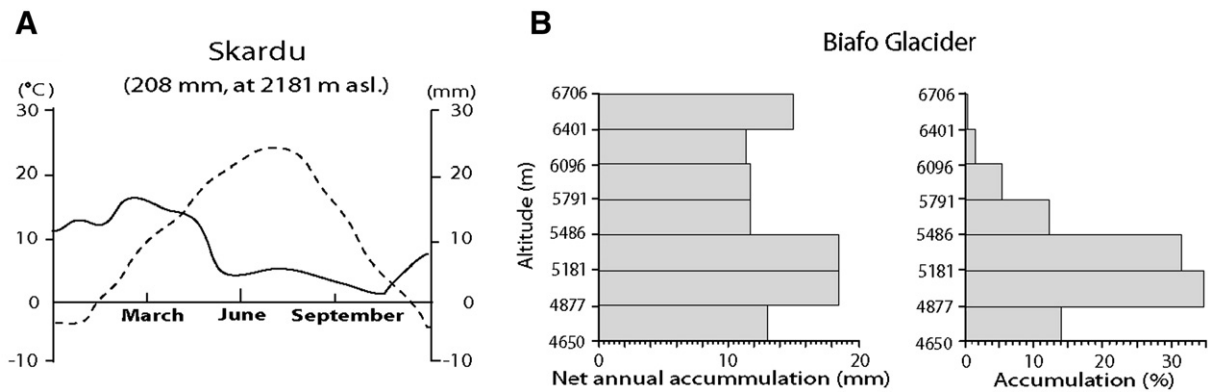


Fig. 4. Climatic characterization of the Central Karakoram. (A) Annual variation of precipitation (solid curve) and temperature (dotted curve) at Skardu. (B) Net annual snow accumulation (mm water equivalent) and percentage accumulation at the accumulation zone of the Biafo Glacier.

The region is currently influenced by two climate systems: the mid-latitude westerlies and the Indian summer monsoon. Microclimatic conditions are highly variable because of complex topography (Owen, 1988; Hewitt, 1989). Over the four decades from 1951 to 1990, the mean annual temperature at Skardu was 11.5 °C and the mean annual precipitation was 208 mm (Fig. 4A; 35°18'N, 75°41'E, 2181 m asl; Mieke et al., 2001). Most of the precipitation falls in spring, when the region receives moisture from the mid-latitude westerlies. According to mass balance data from the Biafo Glacier (36°40'N, 75°57'E, 4650–5520 m asl; Fig. 4B) two-thirds of the annual accumulation of snow in this region is attributed to mid-latitude westerlies during winter, whereas the other one-third comes from the Indian monsoon in summer (Hewitt, 1989). This partitioning in precipitation is also characterized in the snow chemistry on the Biafo Glacier. Wake (1989) found a strong seasonal signal, characterized by relatively higher concentrations of sodium and chlorine in summer snow, indicating that moisture is derived from the Arabian Sea, which was transported to the mountains by summer monsoonal circulation. In contrast, the winter snow is characterized by overall lower concentrations of sodium and chlorine, reflecting moisture derived from distant marine sources, such as the Mediterranean Sea and/or the Atlantic Ocean. The characteristic seasonal climate dominance is also archived in the glacier with $\delta^{18}\text{O}$ estimates from the snow deposited during winter and spring showing more depleted values than in summer snow (Wake, 1987).

A 5- to 10-fold increase in total precipitation occurs between the low-lying dry valley floors and the perennial humid zone of the high peaks (Hewitt, 2005). Thus, the effect of elevation on precipitation results in an altitudinal zonation of vegetation and geomorphic processes (Paffen et al., 1956; Hewitt, 1989, 2005). Natural vegetation is scarce along the valley floors and on the lower valley side slopes, which are of desert type. This is replaced at higher levels (>3000 m asl) by temperate coniferous trees and then by alpine meadow vegetation (>4000 m asl). The precipitation is sufficient to support large glaciers above the altitudes of the alpine meadows. Glaciogeologic evidence indicates the region has experienced at least four major glaciations that include at least six glacial advances (Seong et al., 2007; Table 1).

3. Methodology

Field work was conducted in the valleys from Skardu to the base of K2 during the summer of 2005. Within this region, four areas were selected for geomorphic mapping, sediment logging, and TCN surface exposure dating. These are, in order of increasing altitude upvalley: the Skardu Basin; the Shigar Valley; the Braldu Valley; and the Baltoro Glacier (Fig. 2C). The four areas contain the most extensive and best-preserved depositional landforms, exposed sedimentary sections, and well-preserved moraines, as well as excellent sites for TCN surface exposure dating. In addition, geomorphological and glaciological observations

were obtained on the Biafo, Liligo, and Baltoro glaciers. This included measurements of debris cover, ablation, ice depth, and ice velocities.

3.1. Geomorphic mapping

Geomorphic mapping was conducted in the field, and GPS measurements and ground photography were used as reference data to facilitate mapping from satellite imagery. In addition, topographic maps (1:25,000 and 1:50,000) of the region supplied by the Government of Pakistan were used to aid identification of landforms. Satellite imagery consisted of Landsat ETM+ data acquired on October 17, 1999 and ASTER multispectral imagery data acquired on August 12, 2000. All multi-spectral data were orthorectified to account for relief distortion.

Topographic information was also utilized to generate landform maps. A digital elevation model (DEM) derived from ASTER data was generated to facilitate morphological characterization of the topography and landform features. DEMs have been widely used for mapping landforms, assessing glaciers, and studying the role of surface processes in landscape evolution. We build on the methods of Duncan et al. (1998), Bishop et al. (2001, 2003), Kääb et al. (2002), Kamp et al. (2005). For the study area, scenes from August 2000 (cloud cover less than 10%) were used to generate absolute DEM employing PCI Geomatica 8.2 software. Thirty-six ground control points were used and data holes were filled with SRTM3 data. The constructed DEM was used to help draw the detailed geomorphic maps of each study region (Fig. 5). To define the dominant geomorphic process in each region, the area of landform types of each mapped region were calculated using the ASTER DEM (Fig. 6, Table 2). A differential global positioning system (GPS) and ground penetrating radar (GPR) were used for measuring the velocity and depth of the glaciers. The supraglacial lakes were identified and sizes were measured with a reference to satellite images.

3.2. Equilibrium line altitudes

Equilibrium-line altitudes (ELAs) have been widely used to infer present and former climatic conditions (Ohmura et al., 1992; Benn and Lehmkuhl 2000; Benn et al., 2005; Owen and Benn, 2005). The geometric calculations for present ELA were made using the ASTER

Table 1

Summary of past glaciation in the Central Karakoram Mountains (after Seong et al., 2007, 2008)

Glacial stage	Timing	Style of glaciation
Askole	Holocene	Tributary valley
Mungo	Lateglacial	Main valley
Skardu	Penultimate/or earlier glacial	Extensive valley
Bunthang	>0.72 Ma	Extensive valley

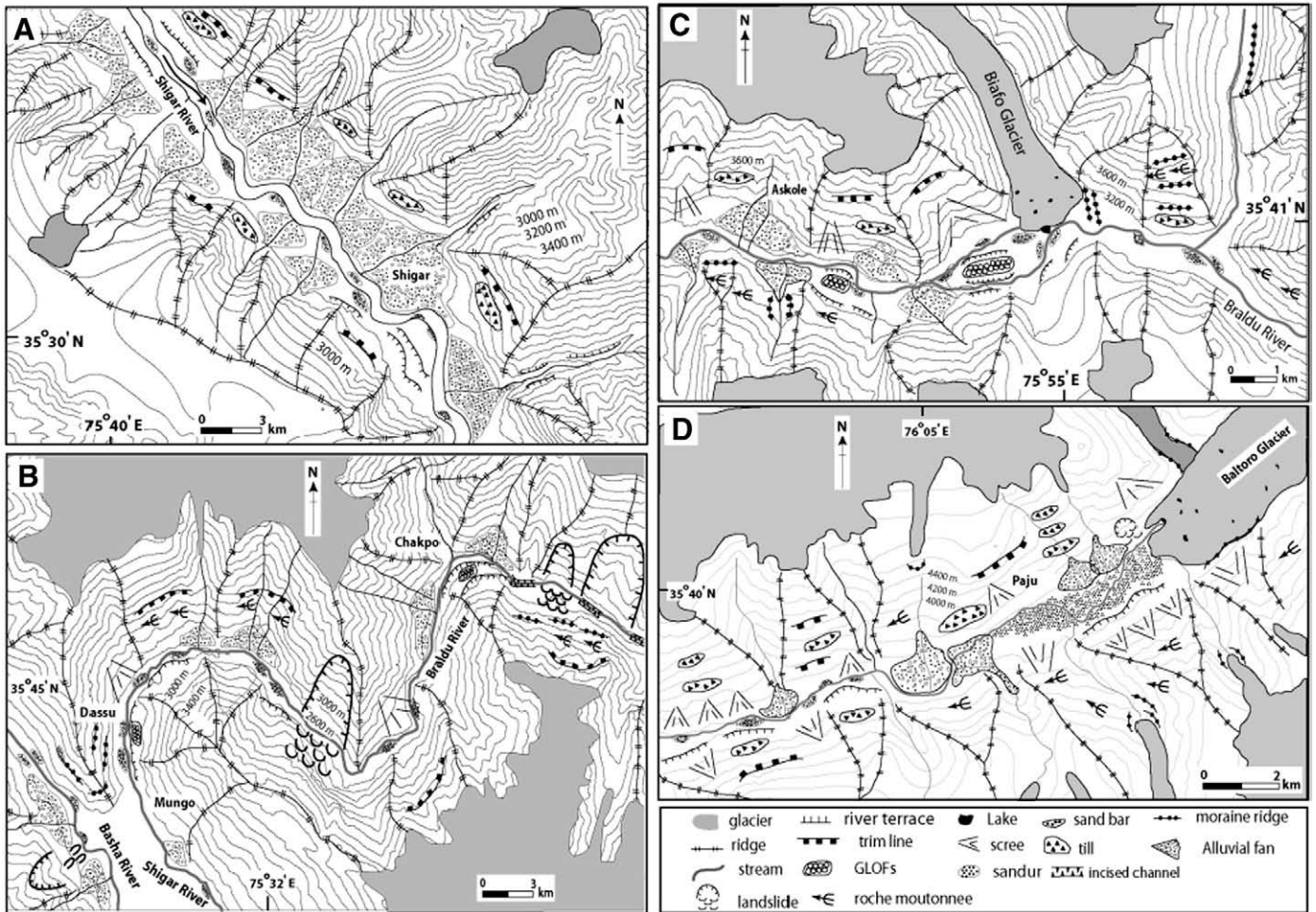


Fig. 5. Geomorphic maps of the study areas. (A) Shigar Valley; (B) Mungo - Dassu - Chapok region valleys; (C) Askole-Biafo region; and (D) Baltoro region (see Fig. 2C for the locations).

DEM (resolution 30 m) and the SRTM imagery (resolution 90 m). Glacial landforms were identified using ASTER and ETM+ satellite images. For modern glaciers, steady-state ELAs should ideally be based on observations of glacier mass balance over several years. Because of the lack of mass balance data, other multiple methods were used that include toe to headwall altitude ratio of 0.5 (THAR), accumulation area ratio of 0.44 and 0.67 (AAR) and balance ratio of 2.0 (BR). Attempts to estimate the ELAs were made for former glaciations only using 0.5 of THAR. Determination of the boundaries of the paleo-glaciers was difficult because of the extensive networks of valley glaciers of small glaciers and snow fields (Seong et al., 2007). The extensive networked valley glaciers have larger accumulation areas supplied from the tributary valley glaciers which likely results in overestimates of the depressions of the past ELAs. The calculated values of the ELAs for the study region are shown in Fig. 7 and Table 3.

3.3. Surface exposure age dating

Samples for TCN surface exposure dating were collected by chiseling off ~500 g of rock from the upper surfaces of quartz-rich boulders in each landform. Locations were chosen where no apparent evidence existed of exhumation or slope instability. The largest boulders were chosen to help reduce the possibility that boulders may have been covered with snow for significant periods (several months) of the year or were previously covered with sediment. To provide a check on the reproducibility of the dating and the possibility of the inheritance of TCNs because of prior exposure to cosmic rays, several (four to seven) samples were collected and dated from each landform. The degree of weathering and site conditions for each boulder were recorded. Topographic shielding was

determined by measuring the inclination from each boulder site to the top of surrounding mountain ridges and peaks.

TCN samples were collected from the top 5 cm of quartz-rich rock to help define the timing of catastrophic events, such as landslides, rock avalanche, and outburst flood deposits. All the samples were prepared in the geochronology laboratories at the University of Cincinnati. First, the samples were crushed using a jaw-crusher and a pulverizer and sieved using standard metric (B.S.) wire mesh sieves. Quartz was then

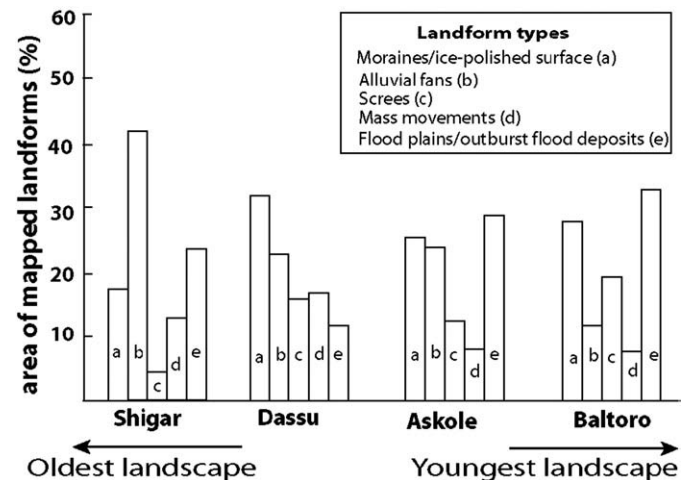


Fig. 6. Area of mapped landform types (in percentage) for the study areas in the Central Karakoram.

Table 2
Area of landforms mapped in the Shigar, Dassu, Askole, and Baltoro valleys

Study area	Total area mapped (km ²)	Total area of mapped landforms (km ²)	Moraines/ ice-polished surface (km ²)	Alluvial fans (km ²)	Screes (km ²)	Mass movements (km ²)	Floodplains/outburst flood deposits (km ²)
Shigar	164.7	51.1	8.7	21.4	2.0	6.6	12.3
(%)			17.0	42.0	4.0	13.0	24.0
Dassu	385.9	108.0	34.6	24.9	17.3	18.4	13.0
(%)			32.0	23.0	16.0	17.0	12.0
Askole	234.4	70.3	18.3	16.9	8.8	6.0	20.4
(%)			26.0	24.0	12.5	8.5	29.0
Baltoro	215.7	49.6	13.9	6.0	9.7	3.7	16.4
(%)			28.0	12.0	19.5	7.5	33.0

The most dominant landform within each area is highlighted in bold.

separated from the 250–500 μm size fraction using the methods of Kohl and Nishiizumi (1992). After addition of ^9Be carrier, Be was separated and purified by ion exchange chromatography and precipitated at $\text{pH} > 7$. The hydroxides were oxidized by ignition in quartz crucibles. BeO was mixed with Nb metal and loaded onto targets for the determination of the $^{10}\text{Be}/^9\text{Be}$ ratio by accelerator mass spectrometry at the Center for Accelerator Mass Spectrometry in the Lawrence Livermore National Laboratory. Isotope ratios were compared to ICN Pharmaceutical, Incorporated ^{10}Be and NIST (National Institute Standard of Technology) standards prepared by K. Nishiizumi (personnel communication, 1995) and using a ^{10}Be half-life of 1.5×10^6 yr. The measured isotope ratios were converted to TCN concentrations in quartz using the total ^{10}Be in the samples and the sample weights. TCN ^{10}Be concentrations were then converted to a rate of steady-state erosion using sea level high latitude (SLHL) ^{10}Be production rate of 4.98 g of quartz per year (Lal, 1991; Stone, 2000; Balco and Stone, in press). Scaling factors were applied to compensate for altitude-dependent effect in calculating cosmic ray exposure ages (Stone, 1999). Error range for the converted exposure age is shown as one standard deviation (e.g. $20 \text{ m Ma}^{-1} \pm 1\sigma$).

4. Observations

4.1. Glaciers, glacier landforms and glaciation

More than thirty glaciers, longer than 20 km, are present in this region (Fig. 2C). They are glaciologically complex in that the

surrounding topography is highly variable, the glaciers typically cover a relatively large altitude range, the cover of glacier debris can be extensive and debris depths are highly variable, glacier topography is highly variable, and glacier dynamics are significantly affected by individual versus coupled glacier systems. This complexity is demonstrated by the highly varied magnitudes of surface ablation, variability in ice-flow gradients among glaciers, and the relatively large number of surging glaciers (Hewitt, 2005).

In general, the glaciers present in the study area are of winter accumulation type, whereas adjacent Himalayan ranges to the south are of summer accumulation type, reflecting the difference in the dominant climate system (Fig. 4). Annual snow accumulation on the Biafo Glacier ranges from 900 to 1900 mm water equivalent and maximum accumulation occurs over altitudes between 4900 and 5400 m asl (Wake, 1989). Most of the present glaciers are of high activity type with high altitude accumulation zones and relatively low slopes (particularly in the ablation areas) compared to the surrounding topography (Andrews, 1975). They are fed by direct snowfall and extensive snow avalanching from steep slopes. For many glaciers in the region, the areas of ablation and accumulation are separated by steep icefalls or avalanche tracks. In the ablation zone of the Biafo and Baltoro glaciers, the regions of the terminus are covered with extensive debris, which can be as much as 15 m or more in thickness. Deposits of mass movements on the glacier surface dramatically influences the local rate of mass balance because of radiative shielding (Fig. 4B). In addition, the debris depths increase near the terminus,

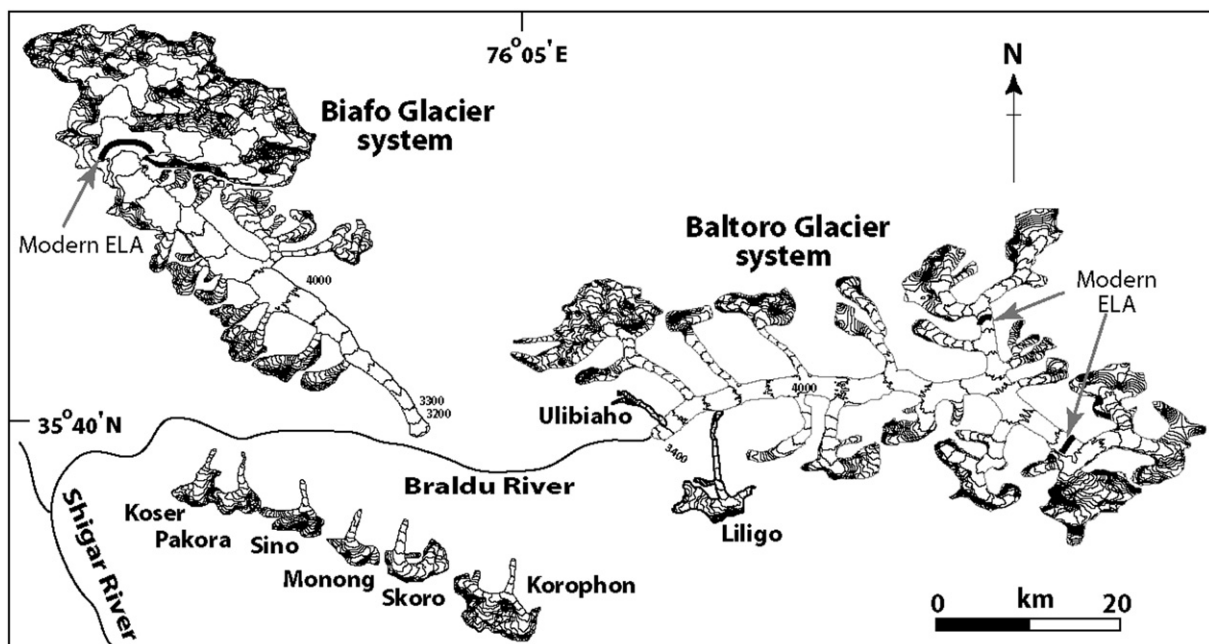


Fig. 7. The main glaciers in the study area showing the topography and present equilibrium line altitudes (shown by the thick black lines).

Table 3
Present and former equilibrium line altitudes (ELAs) for the Central Karakoram

	Present ELAs (m)							Aspect
	Toe (m asl)	Headwall (m asl)	THAR ^a (0.5)	AAR ^b (0.44)	AAR (0.67)	BR ^c (2.0)	Δ ELA for 16 ka (m) ^d	
Biafo	3067	6512	4790	5090	4795	4892		SSE
Ulibiaho	3576	5202	4389	4536	3831	4110		SWW
Liligo	3809	6277	5043	5313	5010	5090		N
Koser	4164	5878	5021	5162	4995	4890		NNE
Pakora	3524	5738	4631	5025	4852	4920		NNE
Sino	3692	5697	4695	4893	4535	4702		N
Monjong	4078	5762	4920	5035	4767	4996		N
Skoro	4146	6180	5163	5117	4854	4924		NNW
Korophon	3946	5761	4854	5070	4876	4910		N
Baltoro	3388	7590	5489	5345	4859	4998	550	W

^a Toe to headwall ratio.

^b Accumulation area ratio.

^c Balance ratio.

^d Toe to headwall ratio of 0.5 used.

and this reduces ablation and permits the glacier terminus to exist at lower altitudes.

Annual ablation of ice between 3500 and 4500 m asl on the Biafo Glacier is of the order of 3000–7000 mm water equivalent (Hewitt, 1989). With increasing altitude the debris cover decreases and facilitates ablation. On the Liligo and Baltoro glaciers, rates of ablation of 65 mm/day (at 3900 m asl) and 59 mm/day (at 4050 m asl), respectively, were measured on exposed ice areas during the summer 2005. The highly variable cover of debris on these glaciers significantly influence the rate of melt and, thus, the velocity of the ice flows. Centerline velocities of ice flow on the Baltoro Glacier were measured in summer 2005 at between 10 m/yr at the glacier terminus (3500 m asl) and a maximum of 245 m/yr at the altitude of 4300 m asl. At altitudes higher than 4500 m asl, velocities gradually decreased to 160 m/yr at K2 base camp (4850 m asl). The high rates of surface melt, combined with crevasses and moulins, produce abundant englacial and subglacial meltwater. The high peak discharges occur in the summer ablation season. The intense melting over 6–10 weeks in the summer releases most of the annual meltwater, producing proglacial landforms such as proglacial lakes and outwash plains (Fig. 8A, B). At the same time, this high summer discharge is likely to destroy the depositional glacial landforms (e.g. terminal moraines) and/or produce catastrophic outburst flood deposits.

At higher altitudes (>5000 m asl), the surface ablation generates significant meltwater, which aggregates to form supraglacial streams and/or ponds (Fig. 8C–F). Much of this water makes it way to the base of the glacier via moulins and fractures which also governs the velocity of the ice. The conditions of the basal water pressure and velocity also influence the erosion potential, and our ice-depth measurements of up to 170 m on the Baltoro Glacier. Such ice thicknesses and high velocities are likely to increase the erosivity of the glaciers. We were unable to obtain, however, clear bed reflection signals in several areas (e.g., Concordia), and so these ice depths must be regarded as minimums. Glacier erosion is expected to be higher in the summer than in the winter, because of significantly higher ablation, basal water pressure, and velocity of the ice.

Impressive successions of moraines and ice-polished surfaces are present downvalley of the margins of most glaciers. Most of the glacial landform associations in the main valleys, such as Shigar and Braldu, are similar to those produced by Pasu-type glaciers of Owen and Derbyshire (1989), which lacks the presence of the extensive ice-contact fans. This probably results from the erosional activity of a migrating glacier meltwater stream and from glacier-outburst flooding. In tributary valleys, however, glacial landform associations of the Ghulkin-type of Owen and Derbyshire (1989), with well-developed ice contact fans and high ridge crested moraines, are present. Extensive glaciofluvial deposits as well as latero-frontal moraines around

Bunthang and Skardu were produced in the past (Fig. 9A, B; Seong et al., 2007). This demonstrates that the style of these glacial landform systems likely changed over time (e.g., the Baltoro Glacier might have changed from a Ghulkin-type to a Pasu-type glacier when it retreated). As a result of the great thickness of the glaciers (Baltoro glacier is >170 m thick), basal sliding is important for producing polished bedrock surfaces and roche moutonnées. The numerous subglacial landforms suggest this characteristic may extend back to the last 20,000 years (Seong et al., 2007; Fig. 9C, D).

Four glacial stages have been recognized in the Skardu-Shigar-Braldu-Baltoro region of the Central Karakoram that includes at least four major and several minor advances (Cronin et al., 1989; Owen, 1988; Seong et al., 2007; Table 1).

4.2. Rivers

The fluvial regime is mainly influenced by the dynamics of glacier meltwater, characterized by large diurnal and seasonal variations in discharge (Hewitt, 1989), although it is well fed during the summer by glacier meltwater and the Indian monsoon rains (Figs. 5 and 10). The Braldu River drains the upstream catchment which consists of the Baltoro, Panmah, and Biafo basins. The Braldu River joins the Basha River to form the Shigar River just south of the village of Mungo. The Shigar River ultimately flows into the Indus River at the town of Skardu. Most of the first- and second-order tributary rivers drain small glaciers and snowfields. Braided streams and incised river gorges are common. Braided streams and outwash plains are present next to glacier margins and in wide valleys, forming valley floors comprised dominantly of cobbly and pebbly bars and swales. These are modified seasonally because of the high variability of discharges. The middle section of the Braldu River, between ~10 km east and west of Chapok, is characterized by deep incision into the bedrock and the development of strath terraces and waterfalls.

The longitudinal profile of the Braldu-Shigar river system shows the typical complex characteristic of a bedrock channel, which consists of three different slope patterns (Fig. 10). The most upvalley reach (upstream of ~10 km east of Chapok) shows incipient, convex shape whereas the most down-valley reach (downstream ~10 km west of Chapok) is characterized by a gentle concave pattern. In contrast, the middle reach, ~10 km west and east of Chapok, exhibits rapid change in the channel gradient, evidenced by a waterfall (<2 m) and a deeply (~40 m) incised gorge. Seong et al. (2008) defines rates incision in fluvial bedrock along the Braldu River by dating strath terraces using ¹⁰Be TCN methods. They showed that Late Quaternary rates of fluvial incisions range from 2 to 29 mm/a, and that the highest rates are in the central gorged section of the Braldu River (a magnitude higher than the upper and lower reaches). They attribute these differences in rates of incision to focused uplift in along the central reach of the Braldu River above the Main Karakoram Thrust.

4.3. Lakes

Several types of lakes are present, formed within hummocky moraines and stagnant ice, or dammed by lateral and frontal moraines in ablation valleys. The largest lake, Satpura Lake (35° 13'49"N, 75° 38'02"E) is over 1.7 km long and 0.9 km wide and occupies a rock basin, which was dammed by either a terminal moraine according to Owen (1988) or a rock avalanche deposit according to Hewitt (1998).

Supraglacial lakes are up to several tens of meters wide and represent a common feature on glaciers in this region (Fig. 8E). The genesis and evolution are complex, and satellite imagery documents significant variation in turbidity conditions, caused from glacier hydrological conditions and ice-flow dynamics. The supraglacial lakes were qualitatively assessed on the Baltoro Glacier, and it appears that the frequency and size of lakes may have increased from 2000 to 2004. Human-induced climate forcing may have helped increased ablation and the presence of

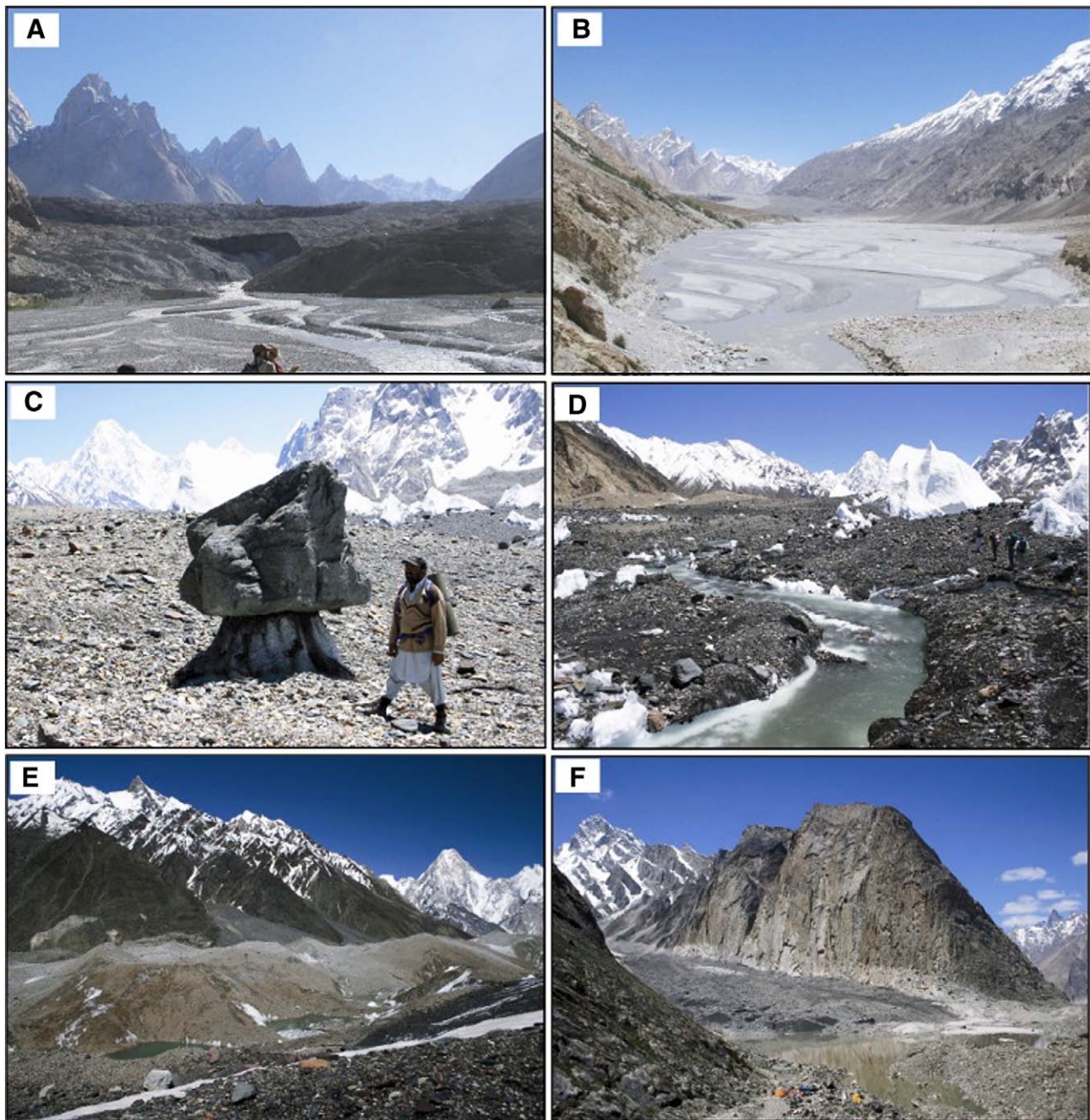


Fig. 8. Examples of glacier types and landforms in the Central Karakoram. (A) View looking at the terminus of the Baltoro glacier covered with thick debris and debris-rich ice. The debris thickness at the terminus is up to 15 m high. (B) View of outwash plain formed in the front of the Baltoro Glacier. (C) A boulder insulating the underlain surface and thus resulting in differential ablation on the glacier surface. (D) Supraglacial channel formed on the Baltoro Glacier. (E) Chains of supraglacial lakes developed on the Baltoro Glacier. (F) Lake Kobuchen dammed by surging of Liligio Glacier. Tents in the foreground are for scale.

surface water on glaciers in this region. Detailed quantitative assessments of these features, and determination of seasonal variation in properties, however, is first required before a definitive conclusion may be drawn.

Where tributary glaciers meet valley trunk glaciers, large supraglacial/ablation valley lakes can form (Fig. 8F). In 1996 Liligio Glacier was observed to have surged to the Baltoro Glacier (Rehmat Ali, pers. comm., 2005) and by 1997 a small lake had formed between the two glaciers (Diolaiuti et al., 2003). Assessments of satellite imagery of the area of the Liligio terminus show that by 3 October 2002 this lake had drained, leaving a light-colored, barbell-shaped sandy plain between the two glaciers. The resultant plain measures ~150–200 m wide (N-S), and ~700 m wide (E-W). A 50–100 m wide sandy runout channel was present and extended all along the left lateral (south) of the glacier margin. By

6 October 2003, two rounded lakes existed at the Liligio terminus; the eastern-most was ~100 m long (N-S) and ~75 m wide (E-W), whereas the western-most was ~75 m in diameter. The two were separated by a ~350 m-wide sandy plain and may have had no, or only limited outflow. By 14 August 2004, the eastern lake was almost at its maximum size (~550 m N-S, ~375 m E-W), and resembled an upright (with respect to north) hook with the shank projecting well out into Baltoro Glacier and the barb pointing east along the valley margin. This lake briefly established an outlet channel several hundred meters across the sand plain and connected to the western lake, as it drained down a crevasse/swallow-hole beneath the Baltoro Glacier. Then by 21 June 2005, the two lakes were reestablished but at a lower level than the prior summer, and with a small outflow only from the western-most swallow-hole.

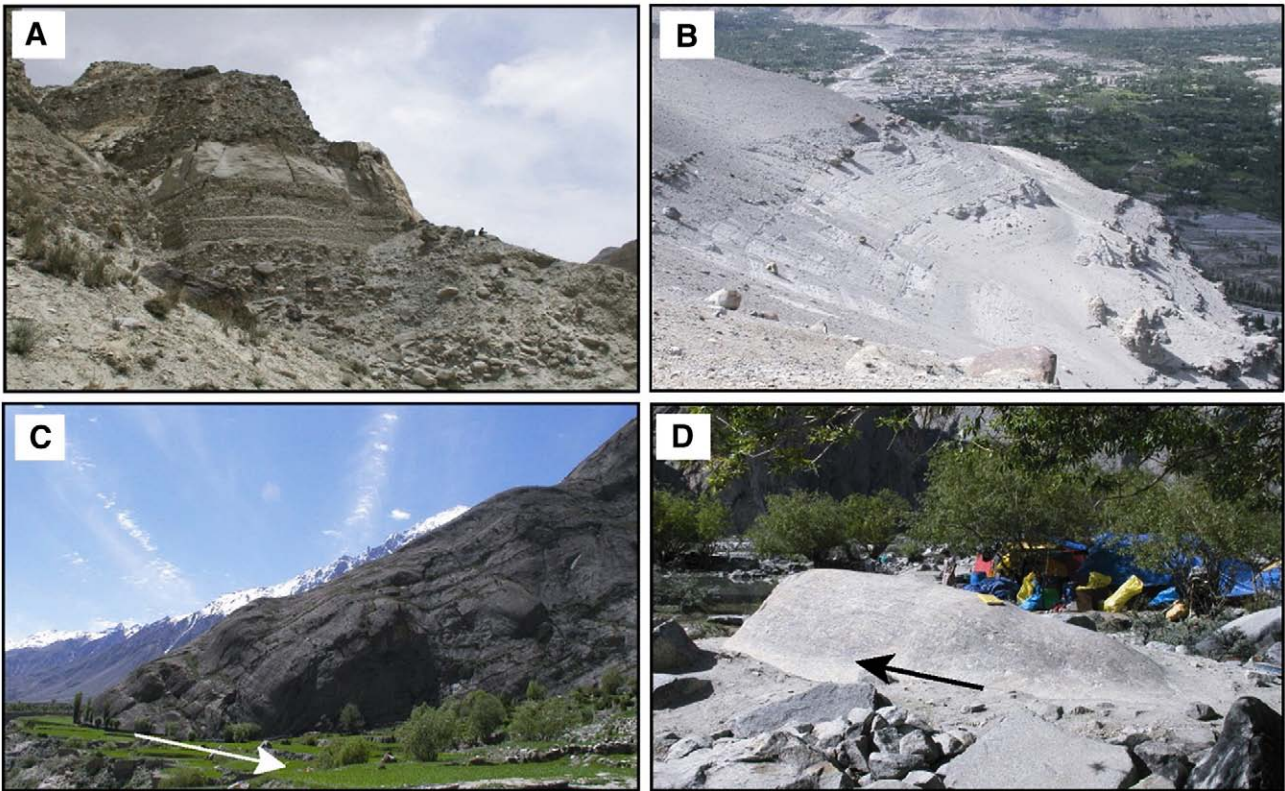


Fig. 9. Depositional and erosional glacial landforms. (A) Well-bedded glacio-fluvial sediments within Bunthang Sequence, ~10 km west of Skardu on the north side of the Indus River. (B) View of stratified lacustrine sediments deposited against Karpochi Rock at Skardu. (C) View looking west of roche moutonnée that was sampled for TCN surface exposure dating around Pakora. The glacier flows out of the photograph. (D) View of whaleback bedform formed by subglacial erosion because of the advance of the Biafo Glacier. The former glacier advanced from the bottom right to the top left.

The following week, on 27–29 June 2005, the continued rise of the eastern lake to shorelines past where it was in the previous summer was observed. The barb of the hook shape extended over a number of porter camps and the main valley side trail was inundated. The water level fluctuated 1–2 m on a diurnal cycle with a daily rise and a nightly

fall. Between then and 16 July 2005 the lake had dropped nearly 10 m and was draining down an ice-bound swallow hole that had migrated upstream from the western lake, across the sand plain between them, and into the west edge of the hook-shaped lake. The decline in Lake-level at that time was measured at ~20–25 cm hr⁻¹. By the morning of

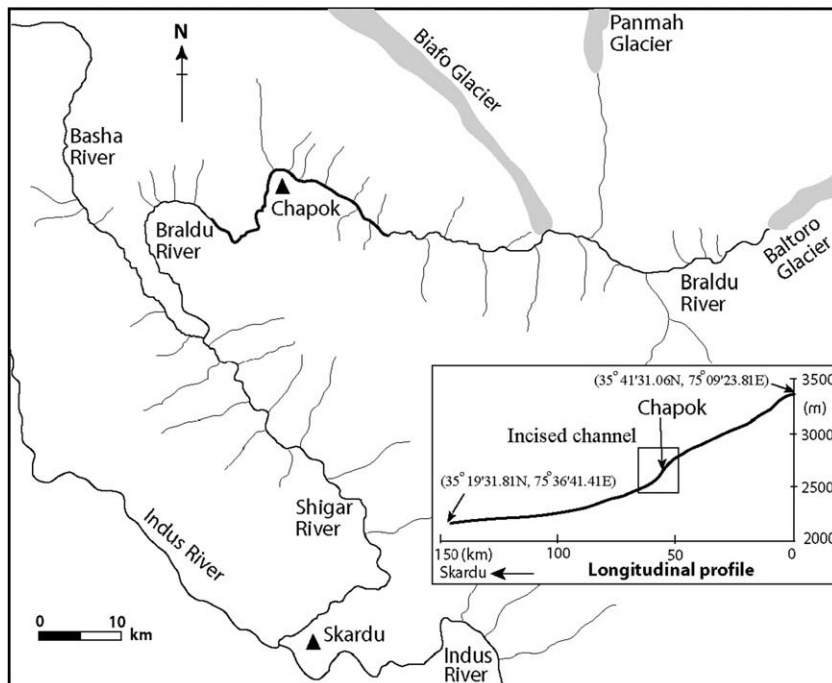


Fig. 10. The main drainages of the study region in the Central Karakoram and longitudinal profile (inset) of Braldu-Shigar River system. Channel gradient is the steepest in the middle reach around Chapok and incised channel pattern is dominant type.

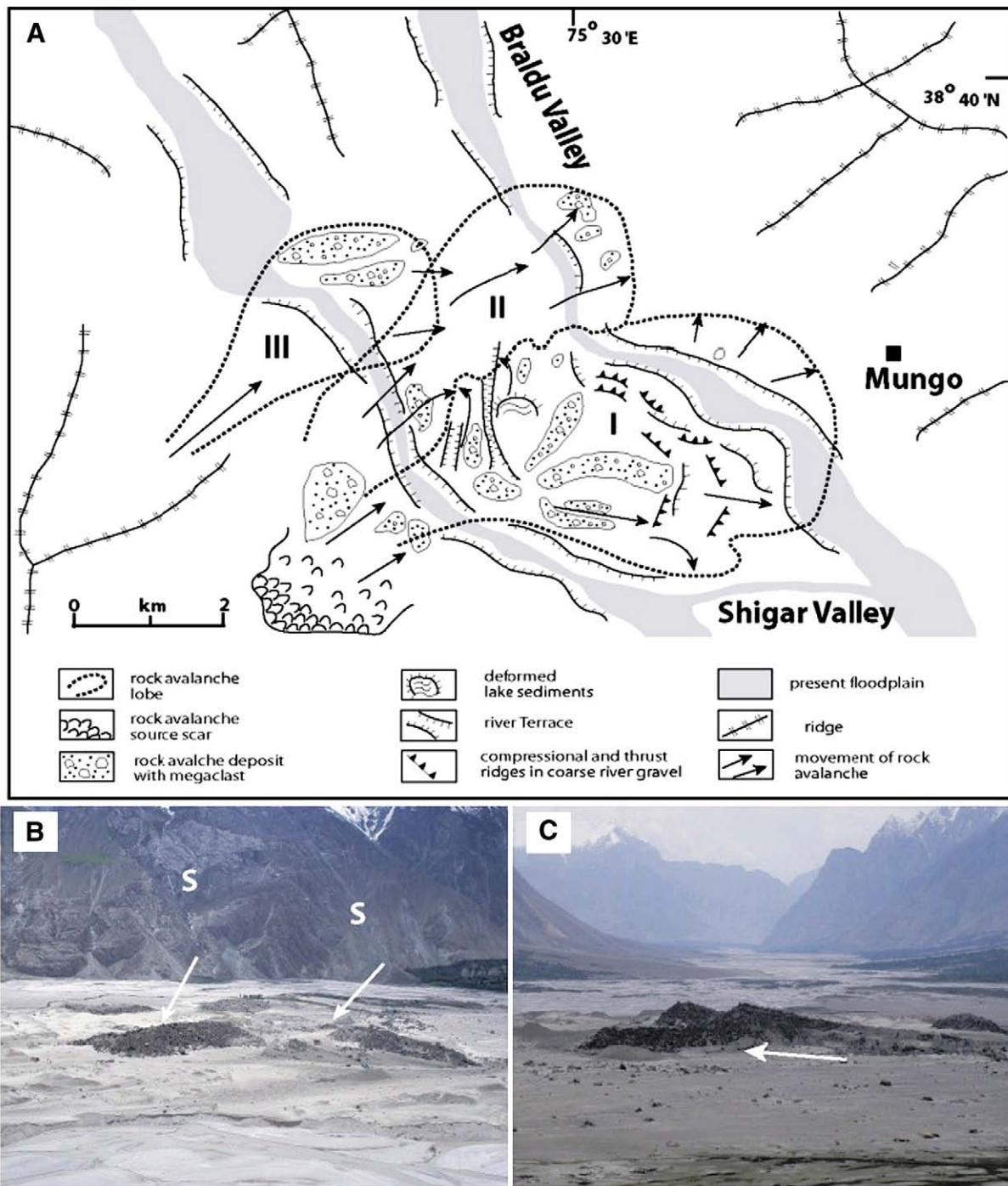


Fig. 11. Selected rock avalanches in the Central Karakoram. (A) The Ghorō-Choh rock avalanches modified from Hewitt (1999). (B) Multiple ridges of rock avalanche deposits. S stands for scoured slope. (C) View looking south from the village of Mungo of deposit of a rock avalanche showing the piled up structure that resulted from high-velocity flow.

17 July the swallow-hole had continued to migrate into the lake and the water level was some meters lower than the previous day. By late July the lake was smaller but had not drained completely because the migration of the swallow-hole was blocked by large immobile boulders. The water descended for some distance into the swallow hole and then reemerged as a glacier marginal stream hundreds of meters farther downvalley, between the Baltoro and the mountain wall where it flowed on the surface for several kilometers, before once again descending beneath the ice.

Lacustrine sediments, numerous in the valleys especially within the middle Indus River, are considered to be related to tributary valley glaciers that blocked the main Indus River (Burgisser et al., 1982;

Derbyshire, 1984; Owen, 1996). Because of the surging character of many glaciers in the region, the formation of ice-dammed lakes by the advance of the tributary glaciers and still is common. Furthermore, large landslides can block alpine valleys and produce large impoundments (Owen, 1996).

4.4. Landslides

Catastrophic landslides and associated landforms are well reported throughout the Karakoram (Hewitt, 1998; Owen, 1989; Hewitt, 1999; Shroder et al., in review). The depositional landforms from mass movement consist of rock falls, debris flow, and snow avalanche deposits.

An impressive deposit form of rock avalanche – identified by Hewitt (1999) and called the Ghoro Choh rock avalanche – exists in the Shigar Valley near the village of Mungo (Fig. 11A). The landform consists of three separate deposits. The prominent ridges of the youngest deposit (Ghoro Choh I) are approximately 20–30 m high and covered by angular megaclasts of up to 10 m in diameter. Most of the boulders are tonalite derived from rock outcrops on the western slope of Shigar Valley. A conspicuous breakout scar (~500 m wide) rises 800–1300 m above the present valley floor. The pile-up structure of the landform blocks and debris indicates multiple avalanches (Fig. 11B and C). The initial rockslide mobilized and incorporated vast quantities of coarse gravels and alluvium in its path. During the avalanching, the underlain floodplain sediments were deformed. Organic material carried within the rock avalanche dates back to the early Holocene (7100 ¹⁴C year). Seong et al. (2007) suggested that a more than 1-km thick valley glacier retreated from the Mungo area by the onset of the Holocene (11,000 years ago). Both results suggest that instability of the slope resulted from postglacial rock debuttressing and likely was the cause of the rock avalanche. See Shroder et al. (in review) for more details.

Another landslide deposit, called the Gomboro rock avalanche by Hewitt (1998), is present in the Braldu Valley near the village of Chapok (Fig. 12). Two main breakout scars are present on the northern slope of the valley (Fig. 12A). The larger one is more than 3 km wide and provided the up to 0.1 km³ of sediments that crossed the Braldu River and were deposited on the southern slope of the valley. Shroder et al. (in review) dated six samples to help define the ages of the landslides. The samples originating from the smaller scar, yielded ages around 14.5 ka (Figs 12B, C; Table 4).

Human-induced landslides are also present in the region but are mainly confined to areas of road construction (Fig. 12D). Failures are most common during the summer season, during or shortly after rain storms, and as a consequence of thawing of any ground ice in spring.

4.5. Alluvial and outwash fans

The steep and unstable valley sides, including bedrock and glacial deposits, provide large volumes of debris that are reworked by streams and debris flows to form active alluvial fans (Fig. 13). Alluvial fans are particularly well formed within the Shigar and Braldu Valley. Throughout the Shigar Valley, they conjugate to form a series of coalescing alluvial fans (bajadas). The alluvial fans, primarily bouldery diamicts and pebbly sands, were mainly deposited by debris flow. They are typically steep (5–10°) and radiate from the narrow valleys.

Alluvial fans on the west side of the Shigar Valley, around the village of Mungo, provide good examples of the relationship between alluvial fans and glacially contributed sediments (Fig. 13A). Here, the alluvial fans are nourished by reworked glacial sediments from the hanging glaciers that are present ~1000 m above them. The glacier and the alluvial fans are connected by the steep surface (>40°) which transfers the sediments. Boulder diamicts dominate the fan surface. The clasts are generally angular and sub-angular and up to 6 m in diameter. The deposits are massive and have an isotropic fabric, although occasionally imbrication and banding is present. Individual beds are up to 2–3 m thick. The channel floor on the fan surface consists of silt- to pebble-sized material reworked by snow and/or glacier meltwater in the ablation season. The fan slopes into the Shigar

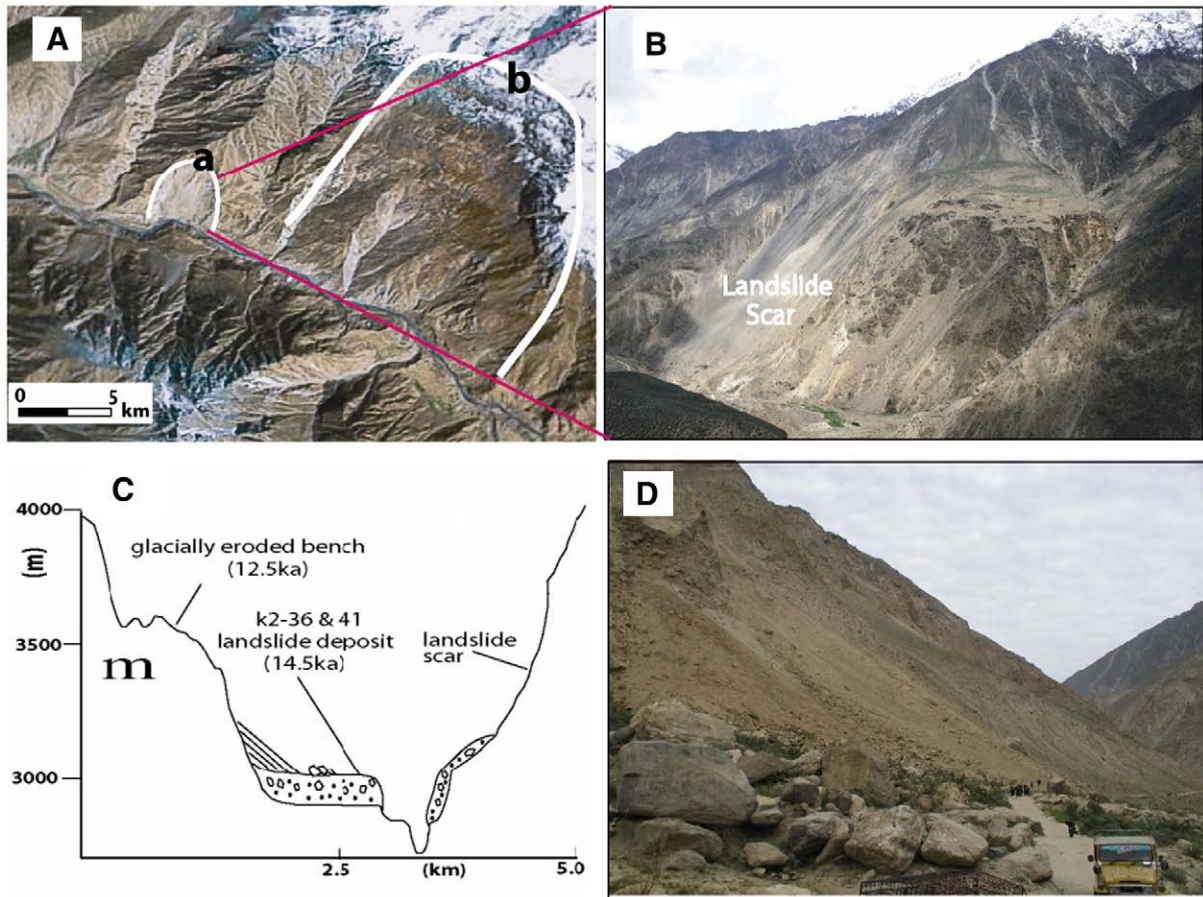


Fig. 12. The Chapok landslides. (A) 3-dimensional view of landslides (from Google Earth). (B) View looking north from the glaciated bench (m) of landslide scar and deposits. The width of the scarred surface measures up to 1 km. (C) Cross-section of the Braldu valley around Chapok showing landslide deposits and glacial landforms. (D) View looking east of landslide which occurred July 12, 2006, and blocked the road.

Table 4
Sampling locations for boulders, landform, topographic shielding factors, ^{10}Be concentrations, and ^{10}Be surface exposure dates

Sample ID	Location	Latitude ($\pm 0.001\text{N}^\circ$)	Longitude ($\pm 0.001\text{E}^\circ$)	Altitude (m asl)	Landform	Shielding factor ^a	^{10}Be (10^4 atoms/g) ^b	^{10}Be Exposure age (ka) ^c
K2-27	Dassu	35.706	75.490	2396	Flood deposit	0.94	15.1 \pm 0.94	6.2 \pm 0.3
K2-28	Dassu	35.707	75.493	2396	Flood deposit	0.94	229.0 \pm 7.10	97.2 \pm 3.0
K2-29	Dassu	35.707	75.491	2396	Flood deposit	0.94	8.42 \pm 0.68	3.5 \pm 0.2
K2-30	Dassu	35.706	75.492	2407	Flood deposit	0.94	3.20 \pm 0.79	1.3 \pm 0.3
K2-106	Chapok	35.739	75.628	2625	Flood deposit	0.97	2.13 \pm 0.70	0.7 \pm 0.2
K2-107	Chapok	35.739	75.626	2624	Flood deposit	0.97	1.96 \pm 0.56	0.6 \pm 0.1
K2-108	Chapok	35.739	75.627	2624	Flood deposit	0.97	2.13 \pm 0.56	0.7 \pm 0.1
K2-109	Chapok	35.739	75.628	2624	Flood deposit	0.97	2.99 \pm 0.48	1.3 \pm 0.1
K2-102	Askole	35.678	75.881	2557	Flood deposit	0.97	4.42 \pm 0.59	1.2 \pm 0.1
K2-103	Askole	35.676	75.880	2950	Flood deposit	0.97	2.59 \pm 0.53	0.7 \pm 0.1
K2-104	Askole	35.675	75.881	2952	Flood deposit	0.97	5.97 \pm 0.62	1.6 \pm 0.1
K2-105	Askole	35.674	75.879	2945	Flood deposit	0.97	6.20 \pm 0.71	1.6 \pm 0.1
K2-36	Chapok	35.729	75.663	2828	Landslide deposit	0.94	46.5 \pm 1.25	14.8 \pm 0.4
K2-37	Chapok	35.729	75.663	2833	Landslide deposit	0.95	47.6 \pm 1.27	14.8 \pm 0.4
K2-38	Chapok	35.729	75.663	2832	Landslide deposit	0.95	48.2 \pm 1.54	15.0 \pm 0.4
K2-39	Chapok	35.730	75.662	2837	Landslide deposit	0.95	46.0 \pm 1.25	14.3 \pm 0.3
K2-40	Chapok	35.730	75.662	2835	Landslide deposit	0.95	46.1 \pm 1.25	14.4 \pm 0.3
K2-41	Chapok	35.729	75.663	2839	Landslide deposit	0.95	40.4 \pm 1.62	12.6 \pm 0.5

Samples K2-36 through K2-41 are taken from Shroder et al. (in review).

^a Shielding factor as calculated to correct for topographic barriers using the methods of Nishiizumi et al. (1989).

^b Atoms of ^{10}Be per gram of quartz before application of shielding correction factor.

^c Minimum ^{10}Be ages were calculated using Stone (2000) scaling factors; sea-level high-latitude (SLHL) production rate = 4.98 ^{10}Be atoms/g quartz per year; zero erosion rate; and sample thickness of 5 cm; asl-above sea level.

River bed, and, thus, the margins of the fan are inundated by the flooding of the Shigar River.

All the alluvial fans are not nourished by glacial sediments. An alluvial fan exposed just north of the village of Mungo, for example, is fed by rock falls and rock avalanches (Fig. 13B). The source area is a very steep slope (30–40°), and gullies, which transport the sediments, lead down to and dissect the fan. The margins of the fan comprise bedded fine sediments formed by flooding of the Braldu River.

4.6. Terraces

A wide range of sediments have been deposited in the valleys and intermontane basins. Many of these deposits have been incised to form the terraces as described in Owen (1989). Different types of terraces are dominated by glacial, lacustrine, mass-movement, fluvial and glaciofluvial sediments (cf. Owen, 1989; Kamp, 2001; Fig. 14). Most of the glacial terraces occupy the upper sections of the valleys close to the present snout of the glaciers. Here, they are better preserved because these valley sections were less exposed to postglacial reworking than the sections down valley (Fig. 14A). Glacial terraces are the result of a modification of subglacial and supraglacial tills, and tills resedimented by mass movement processes.

As mentioned above, lakes and paleolakes of different types are common throughout the Central Karakoram; thus, terraces comprising lake deposits are common. The best example is found in the Bunthang Sequence. Within the sequence, the lake sediments consist of fine-grained clastic sediments, mainly silt size interbedded with imbricated fluvial gravel deposits (Fig. 14B).

Debris terraces, formed by mass movements such as debris flows, rock falls, and rock avalanches, are common throughout the region. The deposits from mass movements, are mainly diamictons, many of which are resedimented deposits of till or previous deposits from mass movements. One example in the Shigar Valley represents multiple sources, such as debris flows and landslides (Fig. 14C).

Fluvial-fill and fluvial-incision terraces are particularly common along the Braldu Valley, comprising poorly sorted sands and gravels. A typical example for a fluvial-incision sequence of terraces is present around the village of Pakora (Fig. 14D). The three terrace levels are a result of down-cutting of the Braldu River (Fig. 14E). The altitudinal decrease of the terraces because of active down-cutting is supported by the gorged reach incised into the bedrock, lying 100 m downvalley

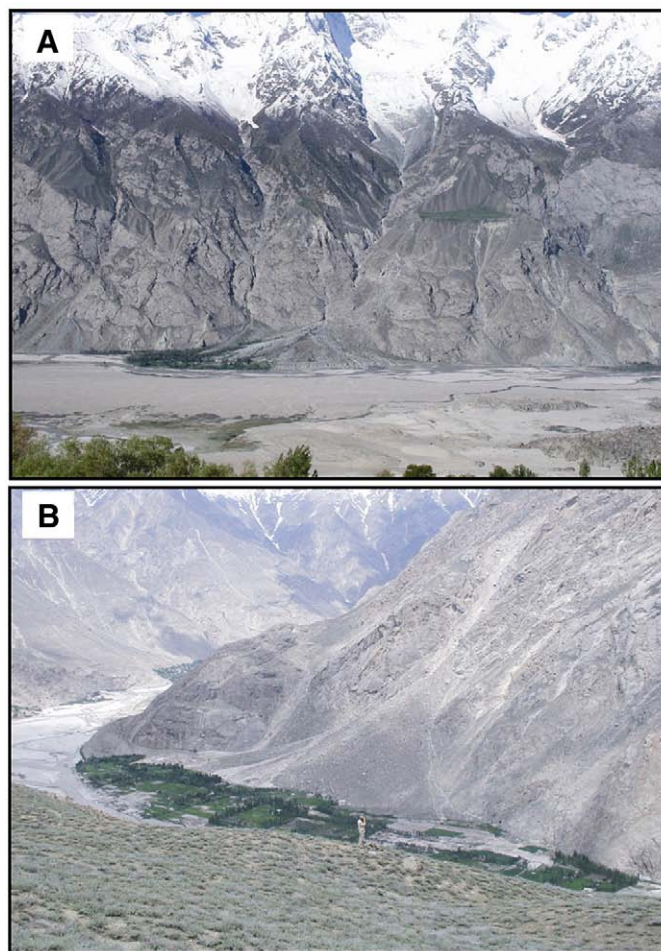


Fig. 13. Examples of alluvial fans in the Central Karakoram. (A) View from Mungo looking west at an alluvial fan fed by glacier and glacial sediments. The river in the foreground is the Shigar River. (B) View northwest at Lower Mungo where the alluvial fan was fed by mass movements, including rock falls and rock avalanches. The village located on the alluvial fan had been destroyed by rock falls and later its inhabitants were evacuated. The Braldu River in the foreground flows to the right out of the picture toward the south.

below the terraces. Active river incision produced rock-cut (strath) terraces (Fig. 14F). Although strath terraces may be produced by relative lowering of base level because of tectonic uplift, it is ambiguous to unravel the relationships between them in the region. Rather, the modern topography of the river bed was likely formed by the glacier when it occupied the valley. After the glacier retreated, the river adjusted to the new topography.

4.7. Flood deposits

Outburst flood deposits are present throughout the entire Braldu Valley up to the present snout of Biafo Glacier (Fig. 15). The source for these deposits could be either landslide blocking or damming by a glacier. The outburst flood deposits in Dassu and Chakpo are likely a consequence of catastrophic landslides, which dammed the Braldu

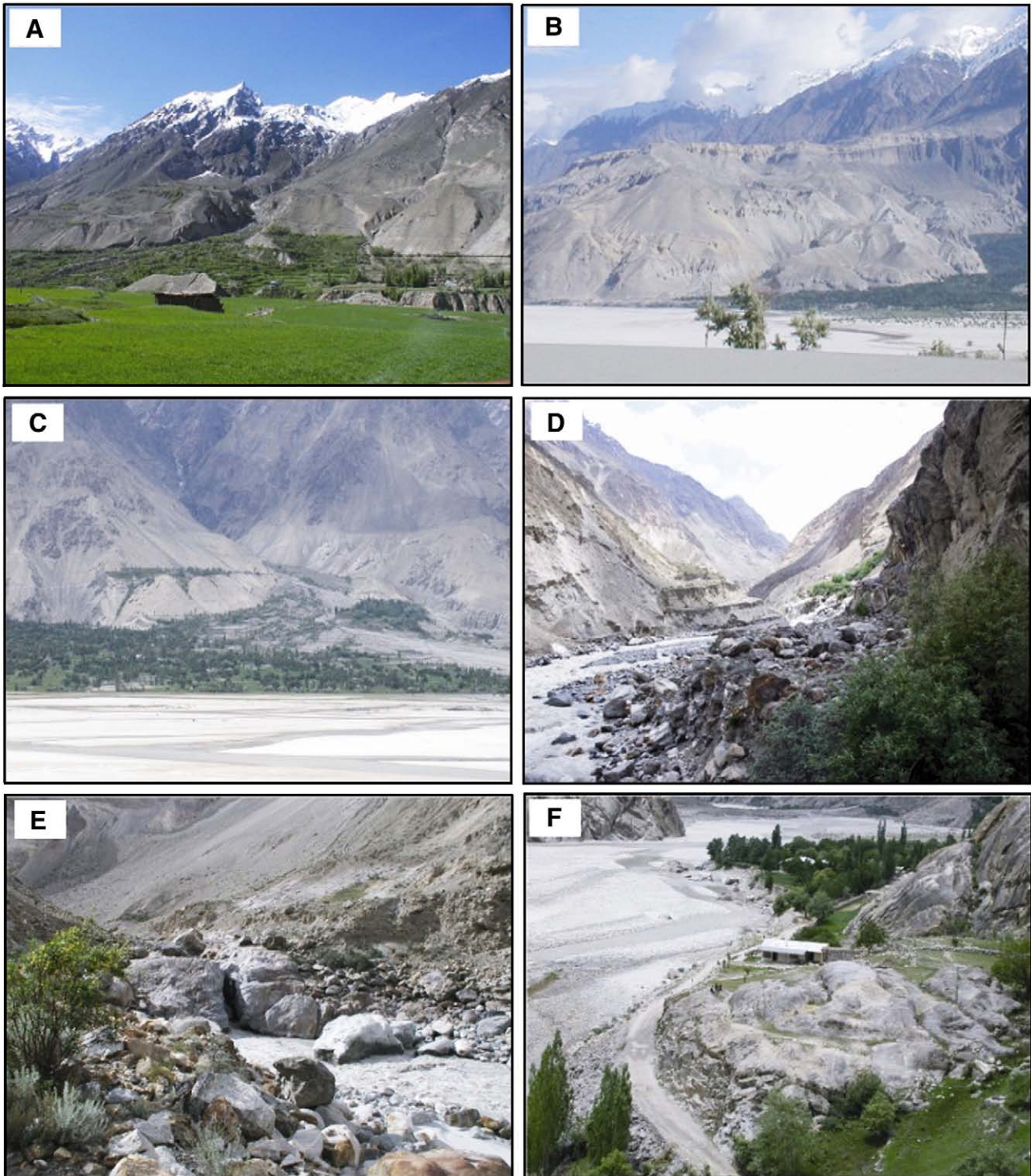


Fig. 14. Examples of terraces in the Central Karakoram. (A) View south from the Askole at glacial terraces formed during Mungo glacial stage. (B) Lacustrine terrace developed within Bunthang sequence. Stratified pale layer is lacustrine sediments. (C) View looking east of debris terrace exposed by erosion of alluvial fan formed by debris flow ~ 5 km north of Skardu. (D) Fluvial terraces formed along the Braldu River around Pakora. Rapid river incision into the fluvial sediments caused the terraces. (E) View of gorged bedrock channel around Chapok. (F) View northwest of rock-cut terraces formed around Dassu. The terraces rise up to 30 m above the present river bed.

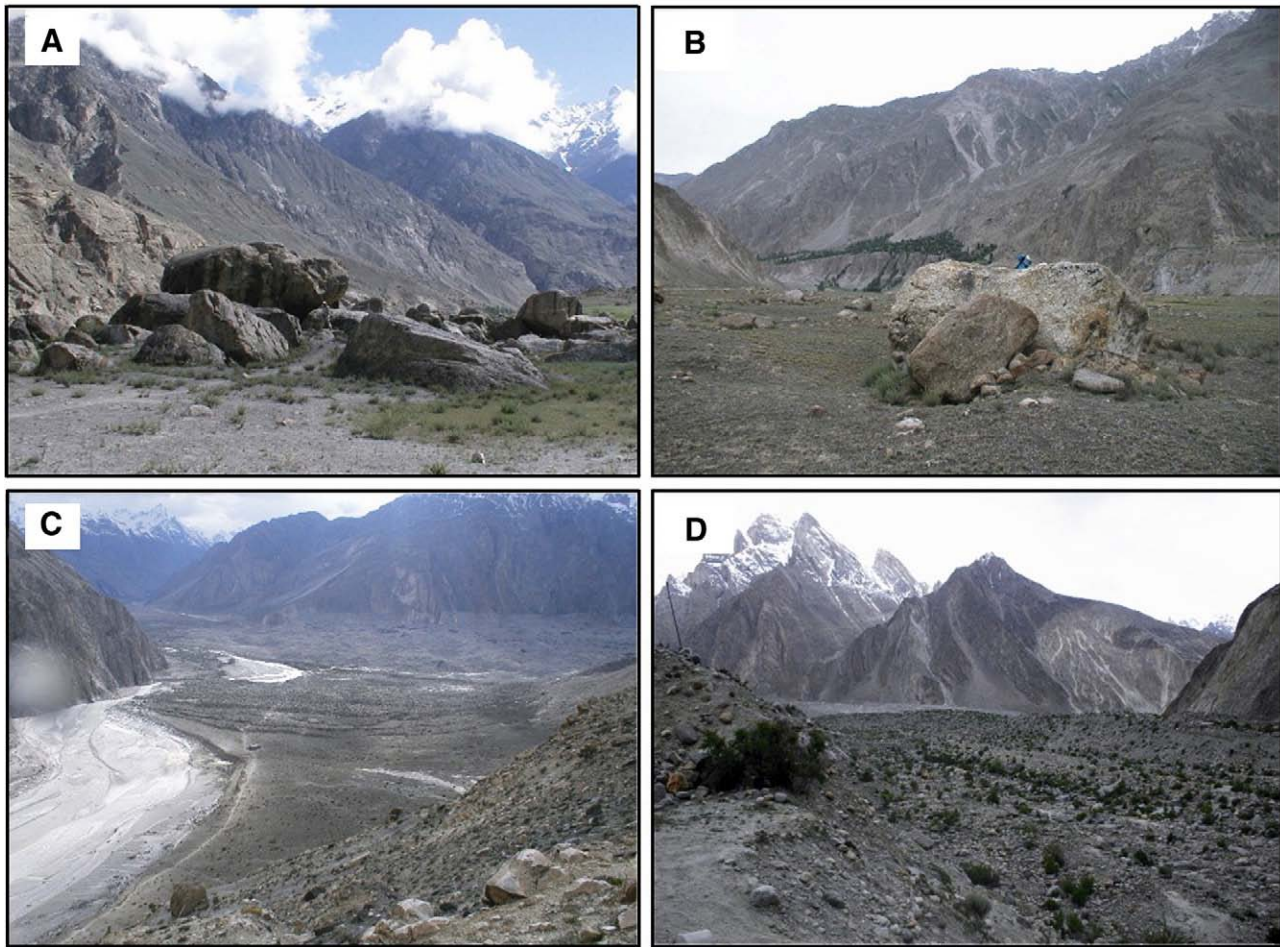


Fig. 15. Flood deposits in the Braldu Valley. (A) View northwest of imbricated mega sized-boulders around Dassu. The boulders measure up to 10 m. (B) View northeast of boulders deposited by outburst flood around 1000 years ago. The backpack on the boulder is for a scale. (C) View southwest of the terminus of the Biafo glacier with multiple lines of lateral moraines. The Braldu River flows through the narrow reach into the picture, which was likely blocked by the Biafo Glacier in the past. (D) View looking northeast towards the front of Biafo Glacier. The gravel- to boulder-size deposits on the terrace in front of mountains are imbricated, suggesting the flow was of high velocity.

River and were subsequently breached (Fig. 15A, B). The valley is very narrow here; therefore, it can be easily dammed. The deposit at Dassu lies approximately 20 m above the present river. The imbricated boulders are up to 10 m in diameter and permit an estimate of the magnitude of the flood (Fig. 15A). Samples from this deposit (K2-27 to K2-30; Table 4) range from 1.3 ka to 6.5 ka. The deposit at Chakpo lies on a terrace approximately 40 m above the present river. The boulders are up to 8 m in diameter and are imbricated. This deposit dates back ~1000 years BP (K2-106 to K2-109). A third deposit from outburst flood is located between Askole and Biafo Glacier. It is likely to be related to a former damming of the Braldu Valley by Biafo Glacier approximately 1500 years ago (K2-102 to K2-105; Fig. 15C, D).

The relationship of flood deposits to glacial and paraglacial processes is reported throughout the Himalayas (Richardson and Reynolds, 2000). Given the TCN surface exposure ages of the deposits and the proximity to landslide deposits, it is reasonable that the described outburst flood deposits in the study area are genetically related to temporary lakes dammed by landslides. All such deposits originated from outburst floods, which can transport large volumes of sediment (Evans and Clague, 1994). Estimates of paleo-flood discharges can be made using empirical and theoretical relationships between boulder size and flow velocity, and the cross-sectional area of the valley using strand line and/or the height of the tallest boulder (Table 5). Empirical functions were, therefore, used to calculate the paleo-velocities that were required to transport the huge boulders (Costa, 1983 [Eqs. (8) and (10)]; Mears, 1979 [Eq. (7)]). The width of the Braldu paleo-channel was measured using a

portable laser distance meter. Paleo-discharges within the channels were calculated from the maximum cross-sectional area and the paleo-velocity based on the boulder size. Most of the floods had discharges in the order of $10^4 \text{ m}^3 \text{ s}^{-1}$. This is similar to values calculated for floods in other regions of the Himalaya (Richardson and Reynolds, 2000).

5. Landscape evolution

The main landforms in this region include rock slopes, moraines, alluvial fans, screes, deposits from mass movements, floodplains and flood deposits. These vary in importance throughout the valleys (Fig. 6). Geomorphological and geochronological evidence reveal that this region has experienced significant glacier fluctuations. The fluctuating climate caused significant glacial expansion and retreat in this region (Seong et al., 2007).

During the Lateglacial (~16 ka), the conjugated Baltoro Glacier system advanced >70 km from the present snout of the glacier and was >1000 m thick at the village of Mungo (Seong et al., 2007). Such thicknesses are based on the lateral moraines and ice-polished bedrock that has been dated. The trunk glacier retreated first from the Shigar Valley and then the Braldu Valley; thus, the former was ice-free much earlier than the latter (Seong et al., 2007). This was followed by less extensive glacial advances during the Holocene (Askole glacial stage) when tributary glaciers advanced down into the upper portions of the Braldu Valley. While the Dassu area has the largest number of primary glacial landforms, fewer such landforms are preserved in the

Table 5

Boulder size data, and paleo-entrainment velocity calculated using the methods of Mears (1979) and Costa (1983) for the flood deposits examined in the Braldu Valley

Location	a-axis (m)	b-axis (m)	c-axis (m)	Entrainment velocity (Costa 1983; Eq. (8)) (ms ⁻¹)	Entrainment velocity (Costa 1983; Eq. (10)) (ms ⁻¹)	Entrainment velocity (Mears 1979; Eq. (7)) (ms ⁻¹)	Mean entrainment velocity (Costa 1983 and Mears 1979 ^a) (ms ⁻¹)	Mean discharge for individual channel sections based on individual boulders and channel cross-sectional area (10 ³ m ³ s ⁻¹)
Dassu	9.0	8.5	3.6	11.0	14.8	11.4	12.4±2.0	19.9±3.3
	6.8	5.7	5.3	9.2	12.1	10.5	10.6±1.5	12.9±1.8
	4.8	3.8	3.2	7.7	10.0	8.5	8.7±1.2	7.5±1.0
	6.8	6.6	6.2	9.8	13.0	11.0	11.3±1.6	13.7±2.0
	7.0	6.1	4.5	9.5	12.6	10.4	10.8±1.6	13.5±1.9
	13.4	9.9	7.5	11.8	15.9	13.8	13.8±2.0	33.0±4.8
	11.2	10.1	10.0	11.9	16.0	13.9	14.0±2.1	27.9±4.1
	7.5	7.4	3.4	10.4	13.8	10.6	11.6±1.9	15.5±2.5
	11.7	6.5	4.0	9.8	12.9	11.7	11.5±1.6	23.9±3.3
	5.3	4.2	4.0	8.0	10.5	9.1	9.2±1.2	8.7±1.2
	5.0	4.1	3.3	7.9	10.3	8.8	9.0±1.2	8.0±1.1
	8.4	4.7	4.5	8.4	11.1	10.4	10.0±1.4	14.9±2.0
	7.7	6.6	5.1	9.8	13.0	11.0	11.3±1.6	15.5±2.2
	5.5	5.5	5.3	9.1	11.9	10.0	10.3±1.5	10.1±1.4
	8.9	5.8	4.7	9.3	12.2	11.0	10.8±1.5	17.2±2.4
	Chapok	7.5	5.4	3.1	9.0	11.8	10.0	10.3±1.4
5.6		5.4	3.2	9.0	11.8	9.4	10.1±1.5	5.8±0.9
5.6		4.1	3.1	7.9	10.3	8.9	9.1±1.2	5.2±0.7
5.2		4.9	3.3	8.6	11.3	9.1	9.7±1.4	5.1±0.8
4.7		3.9	3.8	7.7	10.1	8.8	8.9±1.2	4.3±0.6
7.1		5.9	4.3	9.4	12.4	10.4	10.7±1.5	7.8±1.1
Askole	9.2	7.0	4.2	10.1	13.4	11.2	11.6±1.7	46.9±6.8
	6.0	4.9	3.5	8.6	11.3	9.4	9.8±1.4	25.8±3.6
	6.6	6.5	3.7	9.8	12.9	10.2	11.0±1.7	31.9±5.0
	7.5	5.7	4.8	9.2	12.1	10.6	10.6±1.5	35.1±4.8
	8.2	7.5	4.6	10.4	13.9	11.2	11.8±1.8	42.7±6.5

^a Error is expressed as a standard deviation.

Shigar area, where alluvial fans are the most dominant landform. This is probably because any potential moraines in the Shigar area have been either buried beneath a thick valley fill comprising fluvial and fan sediments or eroded and resedimented by paraglacial processes. Evidence of this reworking is present in the existence of many paraglacial fans. In addition, ice-polished surfaces were eroded by frost weathering and by postglacial bedrock debuttressing, resulting in rock fall or rock avalanches (Figs. 11 and 12).

Moraines and ice-polished surfaces are the most dominant features in the Dassu area, followed by alluvial fans and deposits from mass movements. Glacial landforms are well preserved, particularly between 500 and 1500 m above the present river. This suggests that most of the glacial landforms below this altitude were eroded by mass movement processes after fluvial undercutting and/or resedimented as paraglacial fans. Compared to other locations in the study area, Dassu has the largest area covered by deposits from mass movements, suggesting that the slopes have responded greatest to deglaciation within the region. Furthermore, they are likely still responding to deglaciation. In contrast, the Baltoro area has fewer slopes modified by mass movements. In addition, the rapid incision of the Braldu River is responsible for slopes being more susceptible to mass movements. In the Askole and Baltoro areas, relatively little time has passed since the trunk valley was filled with a thick glacier, and hence paraglacial fans are less well developed.

The degree of glaciation was quantified by calculating the former ELAs. Fig. 7 and Table 3 show the present and former ELAs (at ~16 ka) using multiple methods. The determinations of the ELAs for contemporary glaciers show small variations because of possible micro-climatic and topographic controls on the mass balance. No significant difference exists depending on the aspects and glacier type. Thus, ELAs might play an important role in reconstructing the paleoclimate in the region. The ELA depression (based on a THAR of 0.5) during a Lateglacial advance at ~16 ka was ~550 m in the Central Karakoram.

Multiple glaciations likely put an upper limit on the topographic development in the Central Karakoram, which experienced rapid uplift

over the last 5 million years. The study area represents the mode altitude between 4000 and 5000 m asl (Fig. 3), where modern and late Quaternary dynamic ELAs were at the same range of altitudes. This suggests that glaciers rapidly eroded topography to within this range with remnant peaks extending to higher altitudes. This pattern supports the view that glaciers, facilitated by climate, act as dynamic agents on the surface process and exert a positive feedback on the endogenic process during mountain building process (Zeitler et al., 2001).

The shape and sedimentology of the alluvial fans present in the region are very similar to those described by Derbyshire and Owen (1990) and Barnard et al. (2001, 2003, 2004a,b, 2006). The fans developed by resedimentation shortly after deglaciation. Thus, they are paraglacial in origin. The abundance of these paraglacial landforms suggests that much of the landscape development likely occurred during short time intervals in which the landscape responded to oscillating glaciers. At least five significant glacial advances have occurred during the Late Quaternary. Upon each glacier oscillation, the hydrologic system and associated processes, such as fluvial erosion, fluvial sedimentation and mass movement, would have been dramatically modified. This would have resulted in oscillating sediment transfer and significant landform changes. The importance of paraglaciation has also been highlighted in other regions of the Himalayan-Tibetan orogen and elsewhere in the world (Church and Ryder, 1972, 1989; Fitzsimons, 1996; FitzGerald and Van Heteren, 1999; Curry and Ballantyne, 1999; Curry, 1999, 2000a,b; Bennett et al., 2000; Richardson and Reynolds, 2000; Ballantyne, 2002a,b). Our study, therefore, helps illustrate the importance of paraglaciation in the landscape evolution of glaciated mountains.

Most slopes show major modification by mass movements. The geomorphological maps illustrate the dominance of slope processes and show relationships to glacial landforms. The widespread distribution of paraglacial fans is notable and suggests that mass movement probably intensified during and shortly after deglaciation as large areas of unconsolidated debris were exposed on steep slopes. In addition, the

debutressed bedrock slope, as a result of the pressure of thick ice, is another example of dominant paraglacial processes in the region. Many of the paraglacial landforms, such as rock avalanches, landslides, and deposits from outburst floods are of post-Lateglacial age (Table 4). Episodes of landscape change were probably sporadic and very rapid soon after deglaciation at the end of the Pleistocene.

Catastrophic outburst floods are the result of landslides (Dassu and Chapok) and/or advancing glaciers (Askole). They are efficient at removing a significant amount of sediment out of the system. Catastrophic landslides are widely found throughout the Karakoram (Hewitt, 1998, 1999). Most of them may have been induced by unstable slope failure and large slope failures may even cause subsequent glacier surges (Gardner and Hewitt, 1990; Shroder et al., in review). Consequently strong evidence exists for periodic flooding because of climate change and catastrophic events. Numerous catastrophic outburst floods have occurred during the Holocene in other areas of the Tibetan-Himalaya orogen (Vuichard and Zimmerman, 1986; Hewitt, 1988, 1989; Owen and Derbyshire, 1993; Shroder et al., 1998; Yamada, 1998; Richardson and Reynolds, 2000; Cenderelli and Wohl, 2003). Clearly, these processes constitute a significant factor in the landscape evolution of the Himalaya and Tibet, and likely other high mountain regions.

Collectively, our assessment of landforms and distribution (Figs. 5 and 6; Table 2), along with geochronological results, reveal that climate forcing played a significant role in the landscape evolution of the central Karakoram. Significant changes in climate and glaciation occurred over a relatively short time period, and glaciers were primarily responsible for deeply eroding the landscape. Surface processes readjusted to new environmental conditions after each glacier retreat, and ubiquitous mass movements and catastrophic landsliding further transported material from steep slopes to valley bottoms, while glaciofluvial meltwater and glacier lake outburst floods redistributed sediment down valley. Oscillating glaciers and associated catastrophic mass movements periodically blocked valleys and generated large impoundments of water. These filled large segments of the valleys. High energy catastrophic floods then eroded and transported sediments further down valley and eventually out of the system.

These spatio-temporally overlapping surface processes most likely resulted in relatively high magnitude denudation and relief production. Advances of thick warm-based and polythermal glaciers would result in deep glacier erosion, whereas cold-based glaciers had limited erosion and would effectively protect the landscape. We speculate that significant temporal variations may have occurred in the magnitude of denudation, largely controlled by climate change and glacier fluctuations. To assess the influence of negative mass balance conditions on glacier erosion is more difficult because increased ablation and meltwater could have a significant influence on ice-flow velocities and basal water pressure. In addition, hillslope readjustment to these conditions would also influence the topography, supraglacial debris loads, and therefore, basal rock and shear stress conditions. Nevertheless, denudational unloading would likely have had significant influence on isostatic uplift, and may have caused focused tectonic uplift. Quantifying the magnitude of denudation and the coupling of unloading and uplift is beyond the scope of this paper, but clearly warrants future research.

6. Conclusions

Landform development in the Skardu, Shigar, and Braldu Valleys near K2 in the Central Karakoram is dominated by the influence of glaciation and produced extensive successions of moraines and induced paraglacial modification of the landscape by erosion and resedimentation. The glaciers in this region have oscillated considerably throughout the Late Quaternary, and four glacial stages have been recognized including at least six glacial advances. The extent of glaciation has decreased with time, which has resulted in moraine deposits and ice-polished surfaces. Steep slopes and unstable bedrock and unconsoli-

dated sediments were eroded, transported, and resedimented by non-glacial processes resulting in typical landforms during the readjustment to paraglacial conditions. These include ubiquitous mass movements, catastrophic landslides, and catastrophic outburst floods with peak discharges on the order of $10^4 \text{ m}^3 \text{ s}^{-1}$. These spatio-temporally overlapping surface processes resulted in relatively high-magnitude denudation and relief production. The Holocene ages of the catastrophic events support the view that glaciation likely plays the most important role in the landscape evolution of the Central Karakoram.

Acknowledgements

Our sincere thanks to Dr. Edward Derbyshire and Dr. Marc Caffee for their constructive and helpful comments on our paper. We would especially like to acknowledge the long-term and highly fruitful relationship with the late Syed Hamidullah, former Director of the Centre of Excellence at Peshawar University, who worked so much to help facilitate this project. We would also like to thank his students, Faisal Khan and Mohammad Shahid, for their excellent assistance in the field. This research was supported by funding from the National Geographic Society and the US National Science Foundation (Grant BCS-0242339) to the University of Nebraska-Omaha and the University of Cincinnati. Part of this work was undertaken at the Lawrence Livermore National Laboratory (under DOE contract W-7405-ENG-48). This research forms part of Yeong Bae Seong's doctoral research, which was partially supported by a Meyers Fellowship at the University of Cincinnati.

References

- Andrews, J.T., 1975. *Glacial Systems: An Approach to Glaciers and their Environments*. Wadsworth Publishers Co, Duxbury, London.
- Avouac, J.P., Burov, E.B., 1996. Erosion as a driving mechanism of intercontinental mountain growth. *Journal of Geophysical Research* 101, 747–769.
- Balco, G., Stone, J.O., in press. A simple, internally consistent, and easily accessible means of calculating surface exposure ages or erosion rates from ^{10}Be and ^{26}Al measurements. *Quaternary Geochronology*.
- Ballantyne, C.K., 2002a. Paraglacial geomorphology. *Quaternary Science Reviews* 21, 1935–2017.
- Ballantyne, C.K., 2002b. A general model of paraglacial landscape response. *The Holocene* 12, 371–376.
- Barnard, P.L., Owen, L.A., Sharma, M.C., Finkel, R.C., 2001. Natural and human-induced landsliding in the Garhwal Himalaya of Northern India. *Geomorphology* 40, 21–35.
- Barnard, P.L., Owen, L.A., Finkel, R.C., Asahi, K., 2003. Landscape response to deglaciation in a high relief, monsoon-influenced alpine environment, Langtang Himal, Nepal. *Quaternary Science Reviews* 25, 2162–2176.
- Barnard, P.L., Owen, L.A., Finkel, R.C., 2004a. Style and timing of glacial and paraglacial sedimentation in a monsoonal influenced high Himalayan environment, the upper Bhagirathi Valley, Garhwal Himalaya. *Sedimentary Geology* 165, 199–221.
- Barnard, P.L., Owen, L.A., Sharma, M.C., Finkel, R.C., 2004b. Late Quaternary landscape evolution of a monsoon-influenced high Himalayan valley, Gori Ganga, Nanda Devi, NE Garhwal. *Geomorphology* 61, 91–110.
- Barnard, P.L., Owen, L.A., Finkel, R.C., 2006. Quaternary fans and terraces in the Khumbu Himal south of Mount Everest: their characteristics, age and formation. *Journal of Geological Society of London* 163, 383–399.
- Benn, D.I., Lehmkuhl, F., 2000. Mass balance and equilibrium-line altitudes of glaciers in high mountain environments. *Quaternary International* 65/66, 15–29.
- Benn, D.I., Owen, L.A., Osmaston, H.A., Seltzer, G.O., Porter, S.C., Mark, B., 2005. Reconstruction of equilibrium-line altitudes for tropical and sub-tropical glaciers. *Quaternary International* 138/139, 230–243.
- Bennett, M.R., Huddart, D., Glasser, N.F., Hambrey, M.J., 2000. Resedimentation of debris in an ice-cored lateral moraine in the high-Arctic (Kongsvegen, Svalbard). *Geomorphology* 35, 21–40.
- Bishop, M.P., Shroder Jr., J.F., 2000. Remote sensing and geomorphometric assessment of topographic complexity and erosion dynamics in the Nanga Parbat massif. In: Khan, M., Treloar, P.J., Searle, M.P., Jan, M.Q. (Eds.), *Tectonics of the Nanga Pabat Syntaxis and the Western Himalaya*. Geological Society London Special Publications, vol. 170, pp. 181–200.
- Bishop, M.P., Bonk, R., Kamp, U., Shroder, J.F., 2001. Topographic analysis and modeling for alpine glacier mapping. *Polar Geography* 25, 182–201.
- Bishop, M.P., Shroder Jr., J.F., Bonk, R., Olsenholler, J., 2002. Geomorphic change in high mountains: a western Himalayan perspective. *Global and Planetary Change* 32, 311–329.
- Bishop, M.P., Shroder Jr., J.F., Colby, J.D., 2003. Remote sensing and geomorphometry for studying relief production in high mountains. *Geomorphology* 55, 345–361.
- Brozovic, N., Burbank, D.W., Meigs, A.J., 1997. Climatic limits on landscape development in the northwestern Himalaya. *Science* 276, 571–574.

- Burbank, D.W., Leland, J., Fielding, E., Anderson, R.S., Brozovic, N., Reed, M.R., Duncan, C., 1996. Bedrock incision, rock uplift and threshold hillslopes in the northwestern Himalayas. *Nature* 379, 505–510.
- Burgisser, H.M., Gansser, A., Pika, J., 1982. Late glacial lake sediments of the Indus Valley area, northwestern Himalayas. *Eclogae Geologicae Helveticae* 75, 51–63.
- Cenderelli, D.A., Wohl, E.E., 2003. Flow hydraulics and geomorphic effects of glacial lake outburst floods in the Mount Everest region, Nepal. *Earth Surface Processes and Landforms* 28, 385–407.
- Church, M., Ryder, J.M., 1972. Paraglacial sedimentation: a consideration of fluvial processes conditioned by glaciation. *Geological Society of America, Bulletin* 83, 3059–3071.
- Church, M., Ryder, J.M., 1989. Sedimentology and clast fabric of subaerial debris flow facies in a glacially influenced alluvial fan – a discussion. *Sedimentary Geology* 65, 195–196.
- Costa, J.E., 1983. Paleohydraulic reconstruction of flash-flood peaks from boulder deposits in the Colorado Front Range. *Geological Society of America Bulletin* 94, 986–1004.
- Cronin, V.S., Johnson, W.P., Johnson, N.M., Johnson, G.D., 1989. Chronostratigraphy of the upper Cenozoic Bunthang sequence and possible mechanisms controlling base level in Skardu intermontane basin, Karakoram Himalaya, Pakistan. *Geological Society of America Special Paper* 232, 295–309.
- Curry, A.M., 1999. Paraglacial modification of slope form. *Earth Surface Processes and Landforms* 24, 1213–1228.
- Curry, A.M., 2000a. Observations on the distribution of paraglacial reworking of glacial drift in western Norway. *Norsk Geografisk Tidsskrift* 54, 139–147.
- Curry, A.M., 2000b. Holocene reworking of drift-mantled hillslopes in Glen Doherty, Northwest Highlands, Scotland. *The Holocene* 10, 509–518.
- Curry, A.M., Ballantyne, C.K., 1999. Paraglacial modification of glacial sediments. *Geografiska Annaler* 81A, 409–419.
- Derbyshire, E., 1984. Sedimentological analysis of glacial and proglacial debris: a framework for the study of Karakoram glaciers. In: Miller, K.J. (Ed.), *The International Karakoram Project*, vol. 1. Cambridge University Press, Cambridge, pp. 347–364.
- Derbyshire, E., Owen, L.A., 1990. Quaternary alluvial fans in the Karakoram Mountains. In: Rachocki, A.H., Church, M. (Eds.), *Alluvial Fans: A Field Approach*. Wiley, Chichester, pp. 27–53.
- Diolaiuti, G., Pecci, M., Smiraglia, C., 2003. Lילו Glacier, Karakoram, Pakistan: a reconstruction of the recent history of a surge-type glacier. *Annals of Glaciology* 36, 168–172.
- Duncan, C.C., Klein, A.J., Masek, J.G., Isacks, B.L., 1998. Late Pleistocene and modern glaciations in Central Nepal from digital elevation data and satellite imagery. *Quaternary Research* 49, 241–254.
- Evans, S.G., Clague, J.J., 1994. Recent climatic change and catastrophic geomorphic processes in mountain environments. *Geomorphology* 10, 107–128.
- Fitzsimons, S.J., 1996. Paraglacial redistribution of glacial sediments in the Vestfold Hills, East Antarctica. *Geomorphology* 15, 93–108.
- FitzGerald, D., V. S., 1999. Classification of paraglacial barrier systems: coastal New England, U.S.A. *Sedimentology* 46, 1083–1108.
- Foster, D.A., Gleadow, A.J.W., Mortimer, G., 1994. Rapid Pliocene exhumation in the Karakoram (Pakistan), revealed by fission-track thermochronology of the K2 gneiss. *Geology* 22, 19–22.
- Gardner, J.S., Hewitt, K., 1990. A surge of Bualtar glacier, Karakoram Range, Pakistan: a possible landslide trigger. *Journal of Glaciology* 36, 159–162.
- Hewitt, K., 1988. Catastrophic landslide deposits in the Karakoram Himalaya. *Science* 242, 64–77.
- Hewitt, K., 1989. The altitudinal organisation of Karakoram geomorphic processes and depositional environments. *Zeitschrift für Geomorphologie, N.F. Suppl.-Bd.* 76, 9–32.
- Hewitt, K., 1998. Catastrophic landslides and their effects on the Upper Indus streams, Karakoram Himalaya, northern Pakistan. *Geomorphology* 26, 47–80.
- Hewitt, K., 1999. Quaternary moraines vs catastrophic avalanches in the Karakoram Himalaya, northern Pakistan. *Quaternary Research* 51, 220–237.
- Hewitt, K., 2005. The Karakoram anomaly? Glacier Expansion and the 'Elevation Effect,' Karakoram Himalaya. *Mountain Research and Development* 25, 332–340.
- Kääb, A., Huggel, C., Paul, F., Wessels, R., Raup, B., Kieffer, H., Kargel, J., 2002. Glacier monitoring from ASTER imagery: accuracy and applications. *EARSSEL Proceedings, LISSIG Workshop*, Berne.
- Kamp, U., 2001. Late Quaternary Terraces and Valley Evolution in Chitral, Eastern Hindu Kush. *Zeitschrift für Geomorphologie* 45, 453–475.
- Kamp, U., Bolch, T., O. Isenholzer, J., 2005. Geomorphometry of Cerro Sillajhuay, Chile/Bolivia: Comparison of DEMs Derived from ASTER Remote Sensing Data and Contour Maps. *Geocarto International* 20, 23–34.
- Kohl, C.P., Nishiizumi, K., 1992. Chemical isolation of quartz for measurement of in-situ produced cosmogenic nuclides. *Geochimica et Cosmochimica Acta* 56, 3583–3587.
- Koons, P.O., 1995. Modeling the topographic evolution of collisional belts. *Annual Review Earth Planetary Science* 23, 375–408.
- Lal, D., 1991. Cosmic ray labeling of erosion surfaces: in situ nuclide production rates and erosion models. *Earth and Planetary Science Letters* 104, 429–439.
- Leland, J., Reid, M.R., Burbank, D.W., Finkel, R., Caffee, M., 1998. Incision and differential bedrock uplift along the Indus River near Nanga Parbat, Pakistan Himalaya, from ¹⁰Be and ²⁶Al exposure age dating of straths. *Earth and Planetary Science Letters* 154, 93–107.
- Mears, A.I., 1979. Flooding and sediment transport in a small alpine drainage basin in Colorado. *Geology* 7, 53–57.
- Miehe, G., Winiger, M., Böhner, J., Yili, Z., 2001. Climatic diagram Map of High Asia. Purpose and concepts. *Erdkunde* 55, 94–97.
- Molnar, P., England, P., 1990. Late Cenozoic uplift of mountain ranges and global climatic change: chicken or egg? *Nature* 46, 29–34.
- Montgomery, D.R., 1994. Valley incision and uplift of mountain peaks. *Journal of Geophysical Research* 99, 913–921.
- Nishiizumi, K., Winterer, E.L., Kohl, C.P., Lal, D., Arnold, J.R., Klein, J., Middleton, R., 1989. Cosmic ray production rates of ¹⁰Be and ²⁶Al in quartz from glacially polished rocks. *Journal of Geophysical Research* 94 (B12), 17,907–17,915.
- Ohmura, A., Kasser, P., Funk, M., 1992. Climate at the equilibrium line of glaciers. *Journal of Glaciology* 15, 403–415.
- Owen, L.A., 1988. Wet-sediment deformation of Quaternary and recent sediments in the Skardu Basin, Karakoram Mountains, Pakistan. In: Croot, D. (Ed.), *Glaciotectonics: Forms and Processes*. Balkema, Rotterdam, pp. 123–148.
- Owen, L.A., 1989. Terraces, uplift and climate in the Karakoram Mountains, Northern Pakistan: Karakoram intermontane basin evolution. *Zeitschrift für Geomorphologie* 76, 117–146.
- Owen, L.A., 1996. Quaternary lacustrine deposits in a high-energy semi-arid mountain environment, Karakoram Mountains, northern Pakistan. *Journal of Quaternary Science* 11, 461–483.
- Owen, L.A., Derbyshire, E., 1989. The Karakoram glacial depositional system. *Zeitschrift für Geomorphologie* 76, 33–73.
- Owen, L.A., Derbyshire, E., 1993. Quaternary and Holocene intermontane basin sedimentation in the Karakoram Mountains. In: Shroder, J.F. (Ed.), *Himalaya to the Sea*, London, pp. 108–131.
- Owen, L.A., Benn, D.I., 2005. Equilibrium-line altitudes of the last glacial maximum for the Himalaya and Tibet: assessment and evaluation of results. *Quaternary International* 138, 55–78.
- Paffen, K.H., Pillewizer, W., Schneide, H.J., 1956. Forschungen im Hunza-Karakoram. *Erdkunde* 10, 1–33.
- Parrish, R.R., Tirrul, R., 1989. U-Pb age of the Baltoro granite, northwest Himalaya, and implications for monazite U-Pb systematics. *Geology* 17, 1076–1079.
- Pinter, N., Brandon, M.T., 2005. How erosion builds mountains. *Scientific American Special* 15 (2), 74–81.
- Raymo, M.E., Ruddiman, W.F., Froelich, P.N., 1988. Influence of late Cenozoic mountain building on ocean geochemical cycles. *Geology* 16, 649–653.
- Rex, A.J., Searle, M.P., Tirrul, R., Crawford, M.B., Prior, D.J., Rex, D.C., Barnicoat, A., Bertrand, B.M., 1988. The Geochemical and Tectonic Evolution of the Central Karakoram, North Pakistan. *Philosophical Transactions of the Royal Society of London. Series A, Mathematical and Physical Sciences. Tectonic Evolution of the Himalayas and Tibet*, vol. 326 (1589), pp. 229–255.
- Richardson, S.D., Reynolds, J.M., 2000. An overview of glacial hazards in the Himalayas. *Quaternary International* 65/66, 31–47.
- Robinson, A.C., Yin, A., Manning, C.E., Harrison, T.M., Zhang, S.H., Wang, X.F., 2004. Tectonic evolution of the north eastern Pamir: Constraints from the portion of the Cenozoic Kongur Shan extensional system, western China. *Geological Society of America Bulletin* 116, 953–973.
- Searle, M.P., 1991. *Geology and tectonics of the Karakoram Mountains*. John Wiley & Sons, Chichester, UK.
- Searle, M.P., Parrish, R.R., Tirrul, R., Rex, D.C., 1990. Age of crystallization and cooling of the K2 gneiss in the Baltoro Karakoram. *Journal of the Geological Society of London* 147, 603–606.
- Seong, Y.B., Owen, L.A., Bishop, M., Bush, A., Clendon, P., Copland, L., Finkel, R.C., Kamp, U., Shroder, J.F., 2007. Glacial history of the Central Karakoram. *Quaternary Science Reviews* 26 (25–28), 3384–3405.
- Seong, Y.B., Owen, L.A., Bishop, M.P., Bush, A., Clendon, P., Copland, P., Finkel, R., Kamp, U., Shroder, J.F., 2008. Rates of fluvial bedrock incision within an actively uplifting orogen: Central Karakoram Mountains, northern Pakistan. *Geomorphology* 97 (3–4), 274–286.
- Shroder, J.F., 1998. Slope failure and denudation in the western Himalaya. *Geomorphology* 26, 81–105.
- Shroder, J.F., Bishop, M.P., 1998. Mass movement in the Himalaya: new insights and research directions. *Geomorphology* 26, 13–35.
- Shroder Jr., J.F., Bishop, M.P., Scheppey, R.A., 1998. Catastrophic flood flushing of sediment, western Himalaya, Pakistan. In: Kalvoda, J., Rosenfeld, C.L. (Eds.), *Geomorphological hazards in high mountain areas*. Kluwer Academic Publishers, pp. 27–48.
- Shroder, J., Bishop, M., Bush, A., Copland, L., Kamp, U., Owen, L.A., Seong, Y.B., Weeks, P., in review. Postglacial slope failure and denudation in the Central Karakoram. *Quaternary Science Reviews*.
- Stone, J.O., 1999. A consistent Be-10 production rate in quartz – muons and altitude scaling. *AMS-8 Proceedings Abstract Volume*, Vienna, Austria.
- Stone, J.O., 2000. Air pressure and cosmogenic isotope production. *Journal of Geophysical Research* 105, 23753–23759.
- Vuichard, D., Zimmerman, M., 1986. The Langmoche flash-flood, Khumbu Himal, Nepal. *Mountain Research and Development* 7, 91–110.
- Wake, C.P., 1987. Snow accumulation studies in the central Karakoram. *Proceedings of the Eastern Snow Conference* 44, 19–33.
- Wake, C.P., 1989. Glaciochemical investigations as a tool for determining the spatial and seasonal variation of snow accumulation in the central Karakoram, northern Pakistan. *Annals of Glaciology* 13, 279–284.
- Whipple, K.X., Tucker, G.E., 1999. Dynamics of the stream-power river incision model: implications for height limits of mountain ranges, landscape response timescales, and research needs. *Journal of Geophysical Research* 104, 17661–17674.
- Yamada, T., 1998. *Glacier lake and its outburst flood in the Nepal Himalaya*. Monograph. Data Center for Glacier Research, vol. 1. Japanese Society of Snow and Ice. 96pp.
- Zeitler, P.K., Meltzer, A.S., Koons, P.O., Crow, D., Hallet, B., Chamberlain, C.P., Kidd, W.S.F., Park, S.K., Seiber, L., Bishop, M., Shroder, J.F., 2001. Erosion, Himalayan geodynamics and the geomorphology of metamorphism. *GSA Today* 11, 4–8.